Perozziello, F. & Besozzi, G. (1999) Tuberculosis among immigrants from developing countries in the province of Milan, 1993-1996. *Int. J. Tuberc. Lung Dis.*, **3**, 589-595.

Codecasa, L., Mantegani, P., Galli, L., Lazzarin, A., Scarpellini, P. & Fortis, C. (2006) An in-house RD1-based enzyme-linked immunospot-gamma interferon assay instead of the tuberculin skin test for diagnosis of latent Mycobacterium tuberculosis infection. *J. Clin. Microbiol.*, **44**, 1944-1950.

Das, D., Baker, M., Venugopal, K. & McAllister, S. (2006) Why the tuberculosis incidence rate is not falling in New Zealand. *N. Z. Med. J.*, **119**, U2248.

de Valliere, S., Abate, G., Blazevic, A., Heuertz, R.M. & Hoft, D.F. (2005) Enhancement of innate and cell-mediated immunity by antimycobacterial antibodies. *Infect. Immun.*, **73**, 6711-6720.

Dheda, K., Udwadia, Z.F., Huggett, J.F., Johnson, M.A. & Rook, G.A.W. (2005) Utility of the antigen-specific interferon-gamma assay for the management of tuberculosis. *Curr. Opin. Pulm. Med.*, **11**, 195-202.

Djoba Siawaya, J.F., Beyers, N., van Helden, P. & Walzl, G. (2009) Differential cytokine secretion and early treatment response in patients with pulmonary tuberculosis. *Clin. Exp. Immunol.* **156**, 69-77.

Dosanjh, D.P., Hinks, T.S., Innes, J.A., Deeks, J.J., Pasvol, G., Hackforth, S., Varia, H., Millington, K.A., Gunatheesan, R., Guyot-Revol, V. & Lalvani, A. (2008) Improved diagnostic evaluation of suspected tuberculosis. *Ann. Intern. Med.*, **148**, 325-336.

Ferrara, G., Losi, M., D'Amico, R., Roversi, P., Piro, R., Meacci, M., Meccugni, B., Dori, I.M., Andreani, A., Bergamini, B.M., Mussini, C., Rumpianesi, F., Fabbri, L.M. & Richeldi, L. (2006) Use in routine clinical practice of two commercial blood tests for diagnosis of infection with Mycobacterium tuberculosis: a prospective study. *Lancet*, **367**, 1328-1334.

Geisel, R.E., Sakamoto, K., Russell, D.G. & Rhoades, E.R. (2005) In vivo activity of released cell wall lipids of Mycobacterium bovis bacillus Calmette-Guerin is due principally to trehalose mycolates. *J. Immunol.*, **174**, 5007-5015.

Gordon, S.V., Brosch, R., Billault, A., Garnier, T., Eiglmeir, K. & Cole, S.T. (1999) Identification of variable regions in the genomes of tubercle bacilli using bacterial artificial chromosome arrays. *Mol. Microbiol.*, **32**, 643-655.

Harada, N., Nakajima, Y., Higuchi, K., Sekiya, Y., Rothel, J. & Mori, T. (2006) Screening for tuberculosis infection using whole-blood interferon-γ and mantoux testing among Japanese healthcare workers. *Infect. Control Hosp. Epidemiol.*, **27**, 442-448.

Hunter, R.L., Olsen, M.R., Jagannath, C. & Actor, J.K. (2006) Multiple roles of cord factor in the pathogenesis of primary, secondary, and cavitary tuberculosis, including a revised description of the pathology of secondary disease. *Ann. Clin. Lab. Sci.*, **36**, 371-386.

Jasmer, R.M., Nahid, P. & Hopewell, P.C. (2002) Clinical practice. Latent tuberculosis infection. *New Engl. J. Med.*, **347**, 1860-1866.

Kobashi, Y., Shimuzu, H., Ohue, Y., Mouri, K., Obase, Y., Miyashita, N. & Oka, M. (2009) False negative results of QuantiFERON TB-2G test in patients with active tuberculosis. *Jpn. J. Infect. Dis.*, **62**, 300-302.

Lalvani, A., Nagvenkar, P., Udwadia, Z., Pathan, A.A., Wilkinson, K.A., Shastri, J.S., Ewer, K., Hill, A.V., Mehta. A. & Rodrigues, C. (2001) Enumeration of T cells specific for RD1-encoded antigens suggests a high prevalence of latent Mycobacterium tuberculosis infection in healthy urban Indians. *J. Infect. Dis.*, **183**, 469-477.

Maekura, R., Nakagawa, M., Nakamura, Y., Hiraga, T., Yamamura, Y., Ito, M., Ueda, E., Yano, S., He, H. & Oka, S. (1993) Clinical evaluation of rapid serodiagnosis of pulmonary tuberculosis by ELISA with cord factor (trehalose-6,6′-dimycolate) as antigen purified from Mycobacterium tuberculosis. *Am. Rev. Respir. Dis.*, **148**, 997-1001.

Maekura, R., Okuda, Y., Nakagawa, M., Hiraga, T., Yokota, S., Ito, M., Yano, I., Kohno, H., Wada, M., Abe, C., Toyoda, T., Kishimoto, T. & Ogura, T. (2001) Clinical evaluation of anti-tuberculous glycolipid immunoglobulin G antibody assay for rapid serodiagnosis of pulmonary tuberculosis. *J. Clin. Microbiol.*, **39**, 3603-3608.

Mahairas, G.G., Sabo, P.J., Hickey, M.J., Singh, D.C. & Stover, C.K. (1996) Molecular analysis of genetic differences between Mycobacterium bovis BCG and virulent M. bovis. *J. Bacteriol.*, **178**, 1274-1282.

Mizusawa, M., Kawamura, M., Takamori, M., Kashiyama, T., Fujita, A., Usuzawa M., Saitoh, H., Ashino, Y., Yano, I. & Hattori, T. (2008) Increased synthesis of anti-tuberculous glycolipid immunoglobulin G (Ig G) and Ig A with cavity formation in patients with pulmonary tuberculosis. *Clin. Vaccine Immunol.*, **15**, 544-548.

Mori T. (2000) Recent trends in tuberculosis, Japan. *Emerg. Infect. Dis.*, **6**, 566-568.

Nabeshima, S., Murata, M., Kashiwagi, K., Fujita, M., Furusyo, N. & Hayashi, J. (2005) Serum antibody response to tuberculosis-associated glycolipid antigen after BCG vaccination in adults. *J. Infect. Chemother.*, **11**, 256-258.

Okada, S., Kikuchi, M., Hasegawa, H., Ishikawa, M., Ohno, I., Kaku, M. & Hattori, T. (2002) Delayed recovery of effector memory CD4+ T cells by highly active antiretroviral therapy in a patient with HIV-1 infection. *Tohoku J. Exp. Med.*, **196**, 213-218.

Pai, M., Riley, L.W. & Colford, J.M. Jr. (2004) Interferon-gamma assays in the immunodiagnosis of tuberculosis: a systematic review. *Lancet Infect. Dis.*, **4**, 761-776.

Pereira, S.M., Dourado, I., Barreto, M.L., Cunha, S.S., Ichiara, M.Y., Hijjar, M.A., Goes, J.C. & Rodrigues, L.C. (2001) Sensitivity and specificity of BCG scar reading in Brazil. *Int. J. Tuberc. Lung Dis.*, **5**, 1067-1070.

Turgut, T., Akbulut, H., Deveci, F., Kacar, C. & Muz, M.H. (2006) Serum interleukin-2 and neopterin levels as useful markers for treatment of active pulmonary tuberculosis. *Tohoku J. Exp. Med.*, **209**, 321-328.

van Leeuwen, R.M., Bossink, A.W. & Thijsen, S.F. (2007) Exclusion of active Mycobacterium tuberculosis complex infection with the T-SPOT.TB assay. *Eur. Respir. J.*, **29**, 605-607.

World Health Organization (WHO). (1999) Issues relating to the use of BCG in immunization programs: a discussion document. World Health Organization publication n°. WHO/V 13/99.23., edited by World Health Organization, Geneva, Switzerland.

World Health Organization (WHO). (2007) Global tuberculosis control: Surveillance, Planning, Financing. WHO report. WHO/HTM/TB/2007.376., edited by World Health Organization, Geneva, Switzerland.

World Health Organization (WHO). (2008) Global tuberculosis control; Surveillance, planning financing. WHO/HTM/TB/2008.393., edited by World Health Organization, Geneva, Switzerland.

THE JOURNAL OF IMMUNOLOGY

Potent Antimycobacterial Activity of Mouse Secretory Leukocyte Protease Inhibitor

Junichi Nishimura, Hiroyuki Saiga, Shintaro Sato, Megumi Okuyama, Hisako Kayama, Hirotaka Kuwata, Sohkichi Matsumoto, Toshirou Nishida, Yoshiki Sawa, Shizuo Akira, Yasunobu Yoshikai, Masahiro Yamamoto and Kiyoshi Takeda

J Immunol 2008;180;4032-4039

The Journal of Immunology is published twice each month by
The American Association of Immunologists, Inc.,
9650 Rockville Pike, Bethesda, MD 20814-3994.

Print ISSN: 0022-1767 Online ISSN: 1550-6606.

The Journal of Immunology

Potent Antimycobacterial Activity of Mouse Secretory Leukocyte Protease Inhibitor[1]

Junichi Nishimura,*§ Hiroyuki Saiga,*‡ Shintaro Sato,¶ Megumi Okuyama,‖ Hisako Kayama,*‡ Hirotaka Kuwata,* Sohkichi Matsumoto,‖ Toshirou Nishida,§ Yoshiki Sawa,§ Shizuo Akira,¶ Yasunobu Yoshikai,† Masahiro Yamamoto,‡ and Kiyoshi Takeda[2]*‡

Secretory leukocyte protease inhibitor (SLPI) has multiple functions, including inhibition of protease activity, microbial growth, and inflammatory responses. In this study, we demonstrate that mouse SLPI is critically involved in innate host defense against pulmonary mycobacterial infection. During the early phase of respiratory infection with *Mycobacterium bovis* bacillus Calmette-Guérin, SLPI was produced by bronchial and alveolar epithelial cells, as well as alveolar macrophages, and secreted into the alveolar space. Recombinant mouse SLPI effectively inhibited in vitro growth of bacillus Calmette-Guérin and *Mycobacterium tuberculosis* through disruption of the mycobacterial cell wall structure. Each of the two whey acidic protein domains in SLPI was sufficient for inhibiting mycobacterial growth. Cationic residues within the whey acidic protein domains of SLPI were essential for disruption of mycobacterial cell walls. Mice lacking SLPI were highly susceptible to pulmonary infection with *M. tuberculosis*. Thus, mouse SLPI is an essential component of innate host defense against mycobacteria at the respiratory mucosal surface. ***The Journal of Immunology,*** **2008, 180: 4032–4039.**

Mycobacterium tuberculosis is a top killer among bacterial pathogens and is responsible for 2 million deaths annually. The emergence of AIDS and development of multidrug-resistant *M. tuberculosis* have increased the incidence of tuberculosis, and it has now become a serious problem. Therefore, the host defense mechanisms against *M. tuberculosis* have been intensively investigated and important roles of T cell-mediated adaptive immunity are now well established (1, 2). In addition, functional characterization of TLRs has recently indicated the importance of innate immunity in infection with *M. tuberculosis* (3, 4). Macrophages and dendritic cells are the major effectors of TLR-mediated antimycobacterial immune responses, because they produce a variety of proinflammatory cytokines and have the capacity of phagocytosis. However, during *M. tuberculosis* infection, epithelial cells in the respiratory tract as well as alveolar macrophages are the first targets for invasion by *M. tuberculosis*. Therefore, these epithelial cells are expected to play roles in preventing mycobacterial infection by establishing physical barriers and producing proinflammatory and antimicrobial mediators (5).

Secretory leukocyte protease inhibitor (SLPI)[3] is a 12-kDa secreted protein composed of two cysteine-rich whey acidic protein (WAP) domains (also called WAP four-disulfide core (WFDC) domains) (6–8). It was originally identified in seminal fluid and is produced by secretory cells in the genital, respiratory, and lacrimal glands as well as dermal keratinocytes (9–13). SLPI is a potent inhibitor of serine proteases, such as neutrophil elastase and cathepsin G, and has therefore been proposed to protect tissues from protease-mediated damage at sites of inflammation (14, 15). Indeed, SLPI was subsequently shown to mediate wound healing (16, 17). Further studies have revealed that SLPI has additional functions. For example, it possesses an antimicrobial activities against Gram-negative and Gram-positive bacteria, fungi, and viruses, including HIV (18–20). In addition to SLPI, several other serine protease inhibitors containing a single WAP domain, such as Eppin, Elafin, SWAM1, and SWAM2, also possess antimicrobial activities against Gram-negative and Gram-positive bacteria (8, 21, 22). Thus, serine protease inhibitors possessing WAP domains exhibit antimicrobial activities. However, the precise mechanisms by which these serine protease inhibitors exert their antimicrobial activities remain elusive. More recently, SLPI was found to mediate anti-inflammatory responses. Briefly, SLPI is induced in monocytes and macrophages in response to inflammatory stimuli mediated by TLRs (23) and subsequently suppresses TLR-dependent production of inflammatory mediators in macrophages by modulating NF-κB activity (23–25). Consistent with these findings, SLPI-deficient mice are highly sensitive to TLR4 ligand (LPS)-induced endotoxin shock with increased production of IL-6 (26). Thus, SLPI has diverse functions and its precise roles need to be investigated more carefully.

---

*Deparment of Molecular Genetics and †Division of Host Defense, Research Center for Prevention of Infectious Diseases, Medical Institute of Bioregulation, Kyushu University, Fukuoka; ‡Laboratory of Immune Regulation, Department of Microbiology and Immunology, §Department of Surgery, Graduate School of Medicine, and ¶Department of Host Defense, Research Institute for Microbial Diseases, Osaka University; and ‖Department of Host Defense, Osaka City University Graduate School of Medicine, Osaka, Japan

Received for publication April 3, 2007. Accepted for publication January 9, 2008.

[1] This work was supported by a Grant-in-Aid from the Ministry of Education, Culture, Sports, Science and Technology and the Ministry of Health, Labor and Welfare, as well as the Tokyo Biochemical Research Foundation, the Cell Science Research Foundation, the Yakult Bio-Science Foundation, the Osaka Foundation for Promotion of Clinical Immunology, the Sumitomo Foundation, and the Sankyo Foundation of Life Science.

[2] Address correspondence and reprint requests to Dr. Kiyoshi Takeda, Laboratory of Immune Regulation, Department of Microbiology and Immunology, Graduate School of Medicine, Osaka University, Suita, Osaka, 565-0871, Japan. E-mail address: ktakeda@ongene.med.osaka-u.ac.jp

[3] Abbreviations used in this paper: SLPI, secretory leukocyte protease inhibitor; WAP, whey acidic protein; WFDC, WAP four-disulfide core; qPCR, quantitative PCR; BALF, bronchoalveolar lavage fluid; BCG, bacillus Calmette-Guérin; FLUOS, 5-(6-)carboxyfluorescein-*N*-hydroxysuccinimide ester; NPN, 1-*N*-phenylnapthylamine; AEC, alveolar epithelial cell.

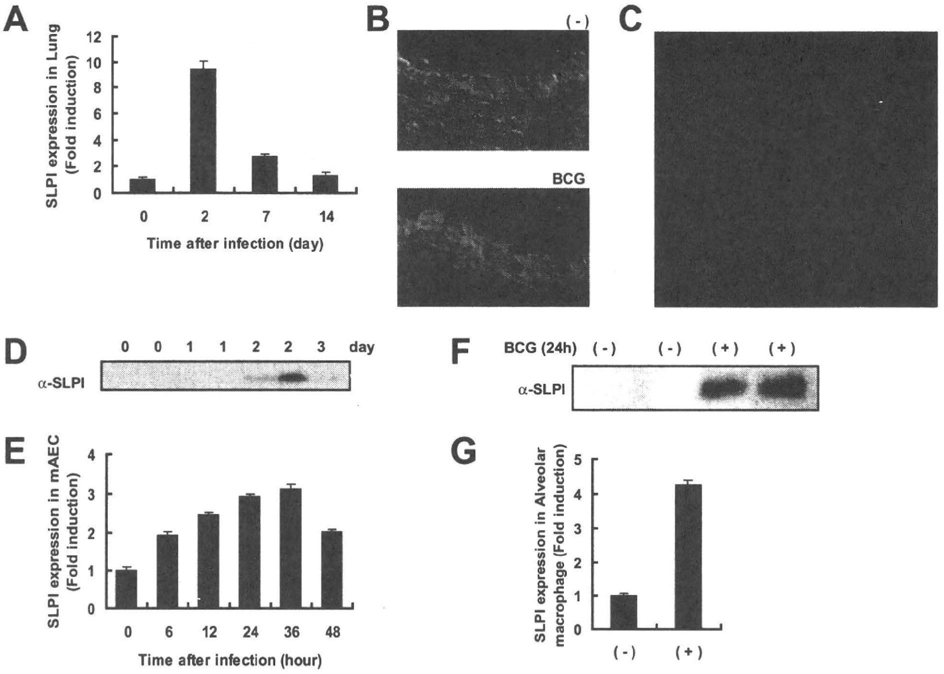

FIGURE 1. Expression of SLPI during mycobacterium infection. *A*, Wild-type mice were intratracheally infected with BCG (4 × 10^5 CFU). At the indicated periods, total RNA was extracted from the lungs. SLPI mRNA expression was analyzed by quantitative real-time RT-PCR. Data are shown as the relative mRNA levels normalized by the corresponding 18S rRNA level. *B* and *C*, At 2 days after intratracheal infection with BCG, lung tissue sections were stained with an anti-SLPI Ab (red) and 4′,6-diamidino-2-phenylindole (blue) and visualized by fluorescence microscopy. *D*, BALF was collected at the indicated periods after BCG infection. Mouse SLPI protein expression was analyzed by Western blotting with an anti-SLPI Ab. Data obtained from two independent mice (0, 1, and 2 days) are indicated. *E*, AEC were incubated with the same number of BCG for the indicated periods. SLPI mRNA expression was analyzed by quantitative real-time RT-PCR. Data are shown as the relative mRNA levels normalized by the corresponding 18S rRNA level. *F*, AEC were incubated with the same number of BCG. Culture supernatants were collected before (−) and after 24 h of infection (+) and subjected to Western blot analysis using an anti-SLPI Ab. Data obtained from two independent cell clones are shown. *G*, Alveolar macrophages were collected from uninfected wild-type mice, cultured with or without BCG for 48 h, and then analyzed for their SLPI mRNA expression by quantitative real-time RT-PCR. The results are presented as the mean ± SD.

In this study, we investigated the roles of murine SLPI in the context of host defenses against mycobacteria, since SLPI expression is greatly induced in macrophages and the lungs during mycobacterial infection (27). Recombinant SLPI inhibited mycobacterial growth at a lower concentration than that required to inhibit bacterial growth. Inhibition of mycobacterial growth was mediated by increased permeability of the mycobacterial membrane. Mutation of cationic residues in the WAP domains of SLPI resulted in loss of its antimycobacterial activity. Furthermore, SLPI-deficient mice were highly susceptible to pulmonary infection with *M. tuberculosis*. These findings demonstrate that SLPI is a potent antimycobacterial molecule.

Materials and Methods

Cells and bacteria

M. tuberculosis strains H37Ra (ATCC 25177; American Type Culture Collection) and *M. tuberculosis* strains H37Rv (28) were grown in Middlebrook 7H9-ADC medium for 2 wk and stored at −80°C until use. *Mycobacterium bovis* bacillus Calmette-Guérin (BCG; Tokyo strain) was purchased from Kyowa Pharmaceuticals. *Salmonella enterica* serovar *typhimurium* were provided by the Research Institute for Microbial Diseases (Osaka University). For each experiment, the dose was confirmed by plating an aliquot of the injected bacterial suspension. Isolation and immortalization of type II alveolar epithelial cells from the lungs of transgenic H-$2K^b$-tsA58 mice were performed as previously described (29), with some modifications.

Immunohistochemistry

Lungs were washed with PBS and frozen in Tissue-Tex OCT compound (Sakura, Tokyo, Japan). Cryostat sections (5-μm thick) were fixed with cold acetone for 10 min, dried, rehydrated with PBS, and blocked with PBS containing 20 mM HEPES, 10% FBS, and 1 μg of Fc-blocking mAb (2.4G2; BD Pharmingen). Next, the sections were sequentially incubated with a biotinylated anti-mouse SLPI Ab (R&D Systems) and Alexa Fluor 594-conjugated streptavidin (Molecular Probes). The nuclei were stained with 4′,6-diamidino-2-phenylindole (Molecular Probes). After washing with PBS, the sections were analyzed by confocal microscopy (Zeiss).

Western blot analysis

Samples were boiled for 5 min in reducing SDS-PAGE sample buffer and then subjected to SDS-PAGE. The separated proteins were transferred to a 0.45-μm pore polyvinylidene fluoride membrane (Millipore). After blocking with 5% milk, the membrane was incubated with the above-described biotinylated anti-mouse SLPI Ab (0.2 μg/ml) and a streptavidin-HRP complex (1/10,000 dilution; R&D Systems). The bound Abs were detected by the Super Signal reagent (Pierce).

Quantitative real-time RT-PCR

After isolation of total RNA with the TRIzol reagent (Invitrogen Life Technologies), 4 μg of the RNA was treated with RQ1DNase (Promega) and then reverse-transcribed using Moloney murine leukemia virus reverse transcriptase (Promega) and Random Primers (Toyobo). Gene expression was quantified with an Applied Biosystems PRISM 7000 sequence detection system using TaqMan Universal PCR Master Mix (Applied Biosystems). To determine the relative expression level of each sample, the corresponding 18S rRNA expression level was measured as an internal control. The primer and probe sequences for SLPI were follows: quantitative PCR (qPCR) primer (forward), 5′-d(GCTGTGAGGGTATATGTGGGAAA)-3′; qPCR primer (reverse), 5′-d(CGCCAATGTCAGGGATCAG)-3′; and qPCR probe, 5′-FAMd(TCTGCCTGCCCCCGATGTGAG)BHQ-3′.

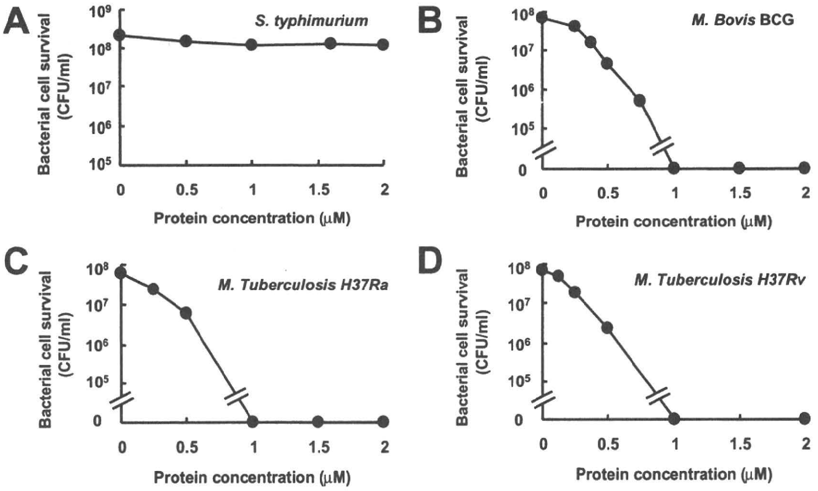

FIGURE 2. Mouse recombinant SLPI inhibits in vitro BCG and *M. tuberculosis* growth. *A*, *S. typhimurium* (5×10^7 CFU/ml) were incubated with SLPI for 2 h and plated on LB agar plates. *B–D*, BCG (*B*), *M. tuberculosis* H37Ra (*C*), or *M. tuberculosis* H37Rv (*D*; 5×10^7 CFU/ml) were incubated with increasing concentrations of recombinant mouse SLPI for 24 h and then plated on 7H10 agar plates.

Bronchoalveolar lavage fluid (BALF)

Mice were intratracheally administered 4×10^5 CFU of BCG suspended in 30 μl of PBS. BALF was collected at the indicated periods. To obtain alveolar macrophages, BALF was centrifuged at 2000 × g for 2 min and the pellet was resuspended in RPMI 1640 containing 4% FBS. The cell count of alveolar macrophages was ~1×10^5 cells/mouse. To eliminate contamination by bacteria, alveolar macrophages were cultured with 50 U/ml penicillin and 50 μg/ml streptomycin for 16 h, washed five times, and infected with 5×10^7 CFU/well of BCG without penicillin and streptomycin.

Preparation of recombinant SLPI protein and variants

PCR-amplified mouse SLPI cDNA fragments were inserted into pGEX-6P-1 (Amersham Biosciences). pGEX-6P-1 containing mouse SLPI cDNA was transformed into *Escherichia coli* Rosetta-gami B (DE 3). Expression of GST-SLPI fusion proteins was induced by the addition of 1 mM isopropyl-1-thio-β-D-galactoside, and the expressed fusion proteins were purified using glutathione-Sepharose 4B (Amersham Biosciences) according to the manufacturer's instructions. The purified proteins were incubated with PreScission Protease (Amersham Biosciences) at 4°C for 16 h to cleave the GST tag and then purified with glutathione-Sepharose 4B.

Antibacterial activity

Mid-log phase *Salmonella typhimurium* were diluted with PBS containing 1% Luria-Bertani (LB) to give ~5×10^7 CFU/ml. A final volume of 250 μl was used to examine the antibacterial activities of proteins. After incubation for 2 h, *S. typhimurium* were plated onto LB agar plates. Colonies were counted (CFU/ml) after overnight incubation at 37°C.

Antimycobacterial activity

M. tuberculosis and BCG were grown in Middlebrook 7H9-ADC medium at 37°C with vigorous agitation. After 7 days of incubation, rapidly growing mycobacteria were harvested by centrifugation and adjusted to 5×10^7 CFU/ml in 7H9-ADC medium. After incubation of the mycobacteria with the indicated concentrations of proteins for 24 h at 37°C, serial 20-fold dilutions were conducted in PBS. Aliquots (50 μl) of the dilutions were plated on Middlebrook 7H10 agar plates and incubated at 37°C for 21–28 days. Colonies were counted (CFU/ml) at intervals until no new colonies appeared.

Protein-binding assay

SLPI and BSA were labeled with 5-(and 6-)carboxyfluorescein-*N*-hydroxysuccinimide ester (FLUOS; Roche Diagnostics) as described previously (30). Briefly, 400 μg/ml SLPI or BSA was mixed with 0.096 mg of FLUOS in 1 ml of PBS for 2 h at room temperature. Nonreacted FLUOS was separated by gel filtration using a Sephadex G25 column (Amersham Biosciences). The labeled SLPI or BSA was then incubated with BCG, and the OD at 630 nm was adjusted to 0.2. After 30 min of incubation at 37°C, BCG were washed three times with 7H9 medium containing 0.05% Tween 80. Protein-BCG reactions were detected by confocal laser microscopy (Zeiss).

Scanning electron microscopy

After culture with or without 1 μM SLPI for the indicated times, BCG cultures were fixed with 5% glutaraldehyde, postfixed with 1% osmium tetroxide, dehydrated with ethyl alcohol, treated with isoamyl acetate to replace the alcohol, dried with liquid CO_2 in a critical-point apparatus (HCP-2; Hitachi), and coated with Pt-Pd by ion sputtering (Hitachi) in ion-distilled water. The specimens were analyzed using S-4700 scanning electron microscope (Hitachi), operated at 10 kV.

Outer membrane permeabilization assay

The ability of proteins to permeabilize the outer membranes of BCG was investigated using 1-*N*-phenylnaphthylamine (NPN; Wako Pure Chemical Industries) as described previously (31). Briefly, BCG were suspended in 5 mM HEPES (pH 7.4) containing 10 μM NPN to an OD at 590 nm of 0.15. After incubation at 37°C for 30 min, proteins were added and the fluorescence of NPN was monitored. The excitation wavelength used was 340 nm, and the emission wavelength was 425 nm. The experiment was conducted at 37°C.

Generation of Slpi$^{-/-}$ *mice*

The *Slpi* gene was isolated from genomic DNA extracted from embryonic stem cells (E14.1) by PCR using TaKaRa LA *Taq*. The targeting vector was constructed by replacing a 1.2-kb fragment containing exons 2–4 with a neomycin-resistance gene cassette (*neo*) driven by the PGK promoter and inserting a HSV thymidine kinase into the genomic fragment for negative selection. After transfection of the targeting vector into embryonic stem cells, colonies resistant to both G418 and ganciclovir were selected and screened by PCR and Southern blotting. Homologous recombinants were microinjected into blastocysts of C57BL/6 female mice and heterozygous F_1 progenies were intercrossed to obtain *Slpi*$^{-/-}$ mice.

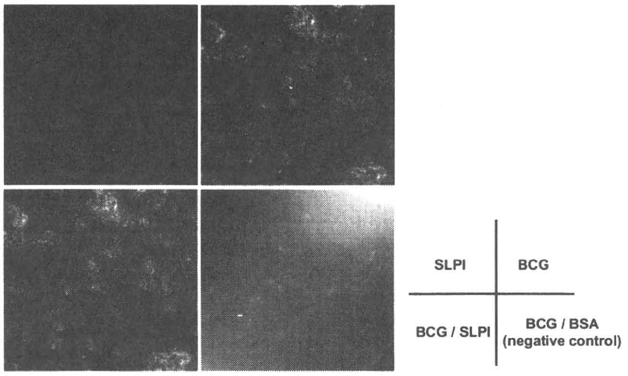

FIGURE 3. SLPI associates with BCG. SLPI and BSA were labeled with FLUOS (Roche). Labeled proteins were incubated with BCG for 30 min, and analyzed by fluorescence microscopy.

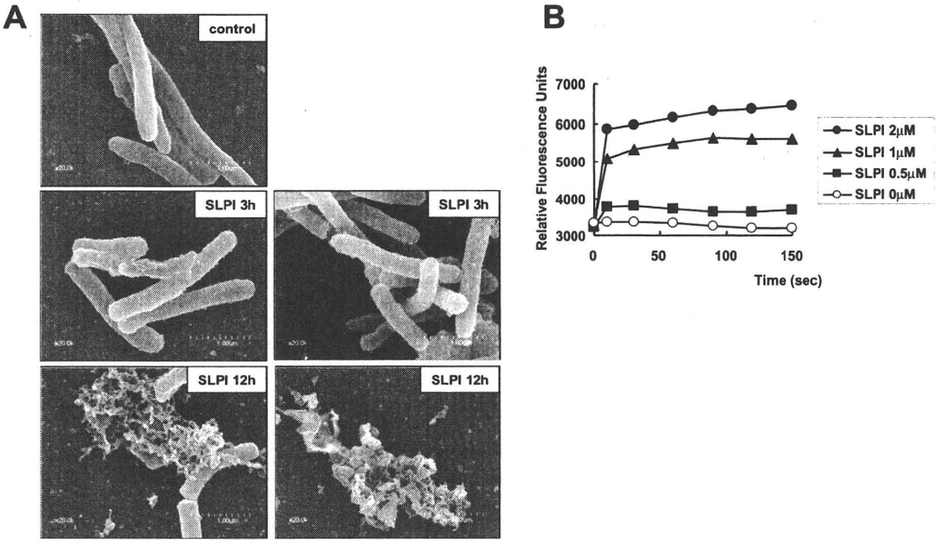

FIGURE 4. SLPI disrupts the BCG cell membrane. *A*, BCG was incubated with or without SLPI for the indicated periods and observed with scanning electron microscopy. *B*, The indicated concentrations of SLPI were added to a BCG suspension containing NPN, and the NPN fluorescence was monitored for the indicated periods. Representative data of three independent experiments are shown.

Slpi$^{-/-}$ mice were backcrossed to C57BL/6 mice for five generations, and *Slpi*$^{-/-}$ and their wild-type littermates from these intercrosses were used for experiments at 6–8 wk of age. All animal experiments were conducted in accordance with the guidelines of the Animal Care and Use Committee of Kyushu University.

In vivo infection

For intratracheal infection, 4 × 10^5 CFU of *M. tuberculosis* suspended in 30 μl of sterile PBS were administered intratracheally. For i.v. infection, 4 × 10^5 CFU of *M. tuberculosis* suspended in 100 μl of sterile PBS were administered i.v. At 3 wk after infection, homogenates of the lungs and spleen were plated on 7H10 agar plates. For histological examination, 1 × 10^7 CFU of *M. tuberculosis* suspended in 30 μl of sterile PBS were administered intratracheally. At 5 days after infection, the lungs were fixed in 4% formalin, embedded in paraffin, cut into sections, and stained with H&E.

Results

SLPI expression in the lungs of BCG-infected mice

To assess the roles of SLPI in mycobacterial infection, we first analyzed SLPI expression in the lungs of mice intratracheally infected with *M. bovis* BCG. Total RNA was extracted from the lungs after 2, 7, and 14 days of infection and analyzed for SLPI mRNA expression by real-time qPCR (Fig. 1*A*). Expression of SLPI mRNA was increased by ~9-fold after 2 days of infection, but decreased thereafter. Next, we analyzed pulmonary cell types expressing SLPI by immunohistochemical analysis (Fig. 1, *B* and *C*). SLPI was detected in bronchial epithelial cells before BCG infection (Fig. 1*B*, *upper micrograph*). After 2 days of BCG infection, increased amounts of SLPI expression were observed, and mainly localized at the apical side of bronchial epithelial cells (Fig. 1*B*, *lower micrograph*). This prompted us to investigate whether SLPI was secreted into the alveolar space after BCG infection. Accordingly, BALF was collected from BCG-infected mice and analyzed for SLPI protein expression by Western blotting (Fig. 1*D*). SLPI was not detected in BALF from uninfected mice. After 2 days of BCG infection, SLPI was abundantly detected in BALF from infected mice, indicating that SLPI was secreted into the alveolar space during the early phase of mycobacterial infection. In addition to bronchial epithelial cells, SLPI was expressed in cells of the alveolar area (Fig. 1*C*). Therefore, we isolated type II alveolar epithelial cells (AEC) and alveolar macrophages and analyzed their SLPI expression levels after BCG infection. Since AEC are difficult to culture in vitro, we took advantage of transgenic mice harboring a temperature-sensitive mutation of the SV40 large tumor Ag gene under the control of an IFN-γ-inducible H-2K^b promoter element (32, 33). Using these mice, we successfully established AEC lines expressing surfactant protein C (data not shown).

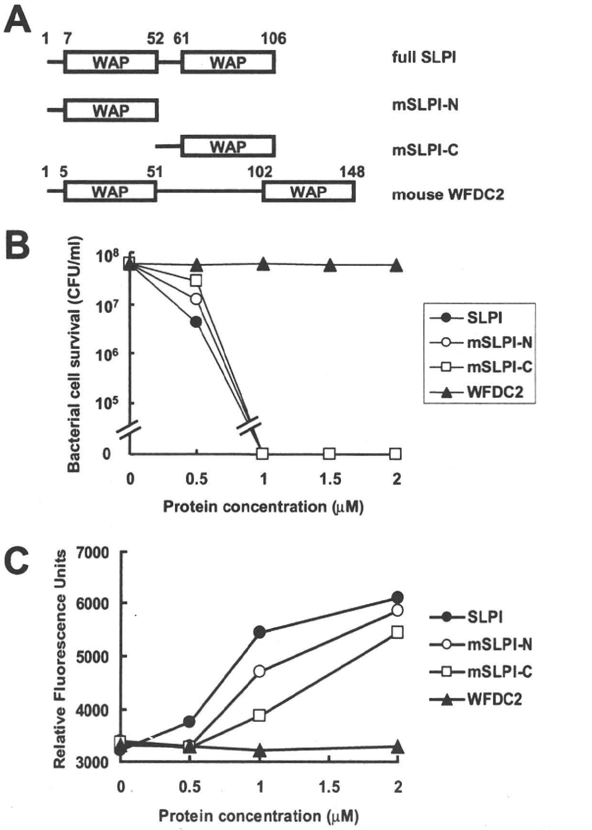

FIGURE 5. A single WAP domain in SLPI is sufficient to inhibit BCG growth. *A*, The deletion mutant constructs mSLPI-N and mSLPI-C lack the C-terminal and N-terminal portions, respectively. White boxes denote WAP domains. *B*, BCG (5 × 10^7 CFU/ml) was incubated with increasing concentrations of the deletion mutants (mSLPI-N and mSLPI-C) or WFDC2 for 24 h and then plated on 7H10 agar plates. *C*, The indicated concentrations of the deletion mutants (mSLPI-N and mSLPI-C) or WFDC2 were added to BCG suspensions containing NPN. The peak of NPN fluorescence within 150 s was plotted. Representative data of three independent experiments are shown.

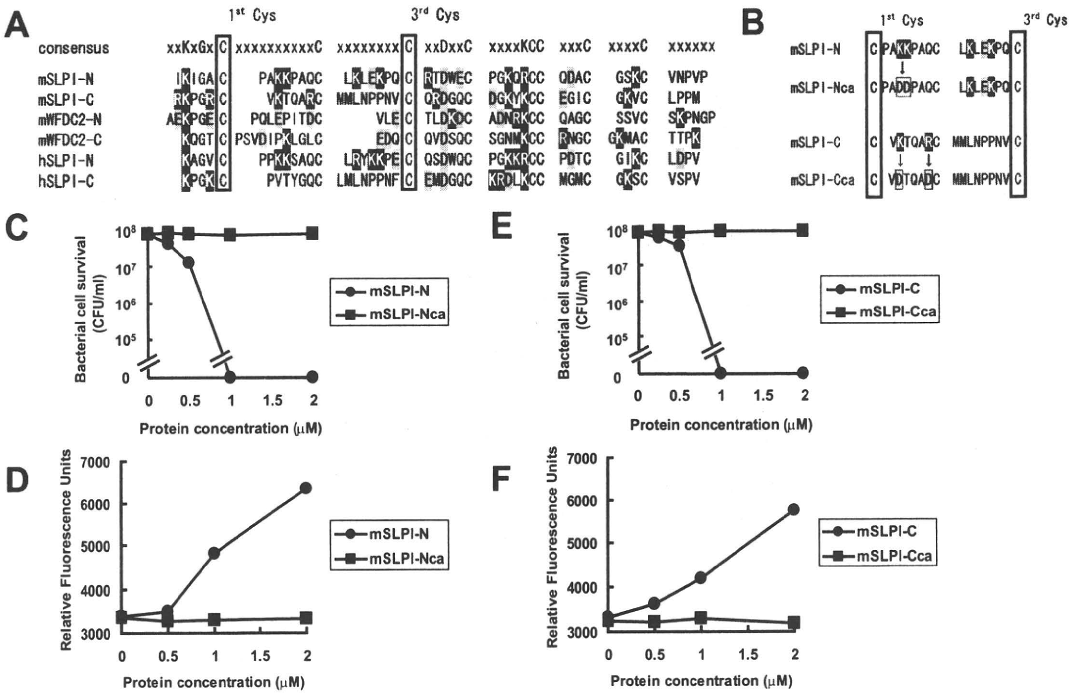

FIGURE 6. Cationic amino acids are responsible for the antimycobacterial activity of SLPI. *A*, Comparison of the WAP domain of SLPI with the WAP domains of other proteins. The consensus amino acid sequence of the WAP domain is shown at the *top* of the protein sequences. Black- and gray-boxed amino acids indicate cationic and anionic amino acids, respectively. Two conserved cysteine residues (first cysteine and third cysteine) are boxed. *B*, Amino acid sequences of the mSLPI-N (mSLPI-Nca) and mSLPI-C (mSLPI-Cca) mutants. *C* and *E*, BCG (5×10^7 CFU/ml) was incubated with increasing concentrations of mSLPI-Nca (*C*) and mSLPI-Cca (*E*) for 24 h and then plated on 7H10 agar plates. *D* and *F*, The indicated concentrations of mSLPI-Nca (*D*) and mSLPI-Cca (*F*) were added to BCG cultures containing NPN. The peak of NPN fluorescence within 150 s was plotted.

AEC were infected with BCG and analyzed for SLPI mRNA expression (Fig. 1*E*). SLPI mRNA expression was gradually induced after BCG infection and peaked after 36 h of infection. AEC have the ability to secrete several effector molecules into the alveolar space. Therefore, we analyzed the SLPI protein levels in culture supernatants from BCG-infected AEC by Western blotting (Fig. 1*F*). SLPI protein was not detected in supernatants from uninfected AEC, but was clearly detected in supernatants after 24 h of BCG infection. Next, isolated alveolar macrophages were infected with BCG and analyzed for SLPI mRNA expression (Fig. 1*G*). BCG infection resulted in an increase in SLPI mRNA expression. Taken together, mycobacterial infection induces the production and secretion of SLPI into the alveolar space by bronchial and type II alveolar epithelial cells as well as alveolar macrophages in the lung.

SLPI-mediated inhibition of mycobacterial growth

Several previous reports have described antimicrobial activities of SLPI against Gram-positive bacteria, Gram-negative bacteria, HIV, and fungi (18–20). However, SLPI needs to be present at high concentrations (>10 μM) for effective inhibition of microbial growth, particularly *S. typhimurium* and *E. coli* (18, 34). Indeed, addition of 2 μM recombinant mouse SLPI only moderately decreased the growth of *S. typhimurium* (Fig. 2*A*). In sharp contrast to the mild inhibition of *S. typhimurium* growth, addition of lower concentrations of mouse SLPI to BCG cultures dramatically reduced the number of CFU (Fig. 2*B*). Growth of BCG was almost completely inhibited by the addition of 1 μM SLPI. A similar inhibitory effect was observed on the growth of *M. tuberculosis* H37Ra and H37Rv (Fig. 2, *C* and *D*). These findings indicate that SLPI has a more potent antimicrobial activity against mycobacteria than against *S. typhimurium*.

Disruption of the BCG cell wall structure by SLPI

Next, we investigated the mechanism of the antimycobacterial activity of SLPI. First, fluorescence-labeled SLPI was incubated with BCG and analyzed by confocal laser microscopy (Fig. 3). BCG and labeled SLPI were colocalized, suggesting that SLPI becomes associated with BCG. We then examined the morphological effects of SLPI on BCG. BCG was incubated with or without SLPI and analyzed by scanning electron microscopy (Fig. 4*A*). BCG exposed to SLPI for 3 h showed pronounced surface blebbing. After 12 h of incubation, many of BCG were collapsed and few live BCG had rough and irregular membrane surfaces. Next, BCG was subjected to an outer membrane permeabilization assay using a fluorescent dye that is weakly fluorescent in aqueous environments but becomes strongly fluorescent in the hydrophobic environment within the cell membrane (Fig. 4*B*). Addition of SLPI caused rapid increases in fluorescence in a dose-dependent manner. These results suggest that SLPI directly associates with mycobacteria, and disrupts the cell wall structure.

Critical role of cationic amino acids in SLPI in its antimycobacterial activity

We next investigated the critical domain involved in the antimycobacterial activity of SLPI. SLPI has two WAP domains (Fig. 5*A*). Several serine protease inhibitors possessing a single WAP domain, such as Eppin, Elafin, SWAM1, and SWAM2, have antimicrobial activities against bacteria such as *E. coli* and *Staphylococcus aureus* (8, 21, 22). To investigate whether each of the WAP domains of mouse SLPI is sufficient to exert antimycobacterial activity, two deletion mutants of SLPI, mSLPI-N and

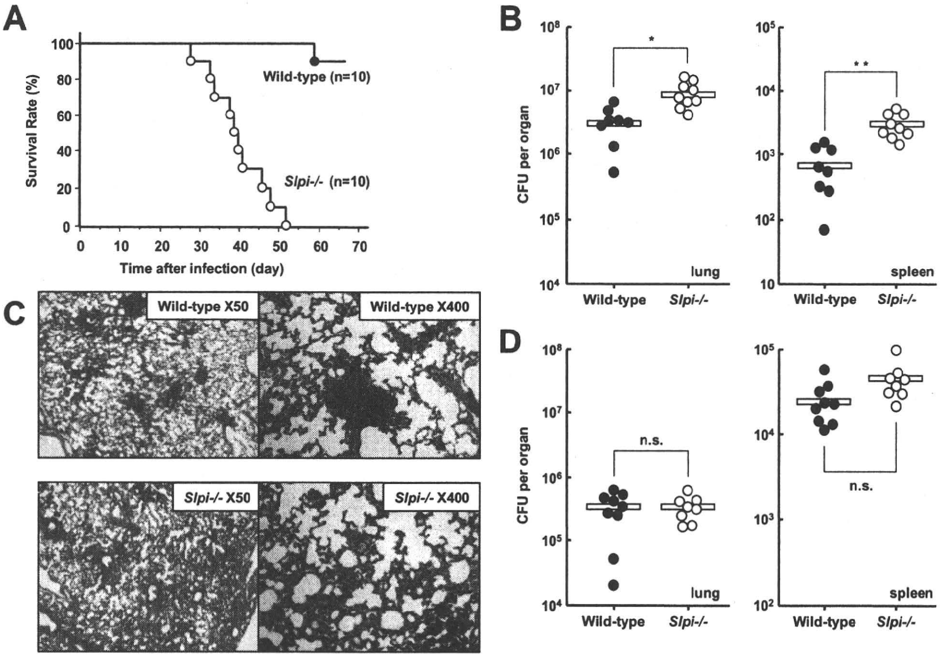

FIGURE 7. *Slpi*$^{-/-}$ mice are highly susceptible to *M. tuberculosis* infection. *A*, *M. tuberculosis* (4×10^5 CFU) were intratracheally infected into wild-type and *Slpi*$^{-/-}$ mice and their survival was monitored. *B*, *M. tuberculosis* (4×10^5 CFU) were intratracheally infected into wild-type and *Slpi*$^{-/-}$ mice. At 3 wk after infection, homogenates of the lungs and spleen were plated on 7H10 agar plates and the CFU titers were counted. Symbols represent individual mice and bars represent the mean of CFU numbers. Statistical analyses were performed using Student's *t* test: *, $p < 0.005$ and **, $p < 0.0005$, significant difference between wild-type and *Slpi*$^{-/-}$ mice. *C*, H&E staining of representative lung tissues from wild-type and *Slpi*$^{-/-}$ mice on day 5 after intratracheal infection with *M. tuberculosis*. *D*, *M. tuberculosis* (4×10^5 CFU) were i.v. infected into wild-type and *Slpi*$^{-/-}$ mice. At 3 wk after infection, homogenates of the lungs and spleen were plated on 7H10 agar plates, and the CFU titers were counted. Symbols represent individual mice and bars represent the mean of CFU numbers. Statistical analyses were performed using Student's *t* test. n.s., Not significant.

mSLPI-C, were generated (Fig. 5*A*). mSLPI-N contained the N-terminal WAP domain, while mSLPI-C contained the C-terminal WAP domain. Both mSLPI-N and mSLPI-C inhibited BCG growth, although their efficiencies were slightly decreased compared with that of full-length SLPI (Fig. 5*B*). Similarly, mSLPI-N and mSLPI-C both induced permeabilization of the outer membrane of BCG with slightly lower efficacies (Fig. 5*C*). These results imply that each WAP domain of mouse SLPI exhibits antimycobacterial activity by disrupting the mycobacterial cell wall structure. WFDC2 is a secreted protein possessing two WAP domains (Fig. 5*A*) (35). However, recombinant mouse WFDC2 had no effect on mycobacterial growth and did not induce permeabilization of the BCG cell membrane, indicating that not all WAP domain-containing proteins have antimicrobial activities (Fig. 5, *B* and *C*). In addition, the N-terminal, but not the C-terminal, WAP domain of human SLPI has been shown to mediate its antimicrobial activities against *E. coli* and *S. aureus* (18). Therefore, we compared the amino acid sequences of the WAP domains of mouse and human SLPI as well as mouse WFDC2 (Fig. 6*A*). The C-terminal regions were conserved among all of the WAP domains. However, the sequences between the first and third cysteine residues were less conserved. In particular, when we examined the sequences between the first and second cysteine residues, we noted that the WAP domains possessing antimycobacterial activities (mSLPI-N, mSLPI-C, and hSLPI-N) contained two or more cationic amino acids, whereas the WAP domains with no antimycobacterial activities (mWFDC2-N, mWFDC2-C, and hSLPI-C) had one or zero cationic acids and instead contained anionic amino acids. Therefore, we produced mSLPI-N (mSLPI-Nca) and mSLPI-C (mSLPI-Cca) mutants, in which the two cationic amino acids were changed to the anionic amino acid aspartic acid (Fig. 6*B*). Neither mSLPI-Nca nor mSLPI-Cca was able to inhibit BCG growth or permeabilize the cell membrane (Fig. 6, *C–F*). These results suggest that the cationic acids of mouse SLPI are responsible for its potent antimycobacterial activities.

High susceptibility of SLPI-deficient mice to M. tuberculosis *infection*

In the next experiment, we assessed the physiological roles of SLPI during mycobacterial infection by generating mice lacking SLPI (*Slpi*$^{-/-}$ mice) via gene targeting (data not shown). First, wild-type and *Slpi*$^{-/-}$ mice were intratracheally infected with *M. tuberculosis* H37Ra, and monitored for their survival (Fig. 7*A*). All *Slpi*$^{-/-}$ mice died within 8 wk of infection at a dose that almost all wild-type mice survived for >9 wk. Next, we counted CFU numbers in the lungs and spleen after 3 wk of infection (Fig. 7*B*). The CFU titers of *M. tuberculosis* in both tissues were higher for *Slpi*$^{-/-}$ mice than that for wild-type mice. The histopathological changes in the lungs after 5 days of *M. tuberculosis* infection were also analyzed (Fig. 7*C*). In wild-type mice, the formation of several small granulomas was observed. In contrast, granulomatous changes were induced to a lesser extent in *Slpi*$^{-/-}$ mice and rather diffuse cell infiltration was observed instead. Next, mice were i.v. infected with *M. tuberculosis*, and the CFU numbers in the lungs and spleen were counted after 3 wk of infection (Fig. 7*D*). The CFU titers were not as dramatically increased in both tissues of *Slpi*$^{-/-}$ mice compared with the corresponding titers in the tissues of wild-type mice, indicating that *Slpi*$^{-/-}$ mice are not highly susceptible to i.v. *M. tuberculosis* infection. Taken together, these findings indicate that *Slpi*$^{-/-}$ mice are highly vulnerable to *M. tuberculosis* infection via the respiratory route.

Discussion

In the present study, we analyzed the roles of mouse SLPI in host defense against mycobacteria. During the early phase of respiratory mycobacterial infection, SLPI was produced and secreted into the alveolar space by bronchial and type II alveolar epithelial cells as well as alveolar macrophages. Recombinant mouse SLPI inhibited the growth of mycobacteria more effectively than it inhibited the growth of Gram-negative bacteria. The SLPI-mediated inhibition of mycobacterial growth was attributable to disruption of the mycobacterial cell wall structure. Furthermore, $Slpi^{-/-}$ mice were highly susceptible to pulmonary *M. tuberculosis* infection, highlighting a mandatory role for mouse SLPI in the host defense against *M. tuberculosis* infection. Thus, mouse SLPI is a critical antimycobacterial molecule that acts during the early phase of mycobacterial infection at the respiratory mucosal surface.

Similar structural changes to those observed in SLPI-treated mycobacterial cell walls were induced in several bacteria and *M. tuberculosis* treated with the antimicrobial peptides defensins, which permeabilize microbial membranes (36, 37). We further identified the critical elements for the potent antimycobacterial activity of mouse SLPI. It has been proposed that defensins containing positively charged amino acid residues associate with microorganisms by targeting the surface-exposed negatively charged phospholipid head groups in the microbial membrane (37). Indeed, mutations that change arginine to aspartic acid can attenuate the bactericidal activity of the α-defensin cryptdin-4 (38). Therefore, we supposed that SLPI, which has similar effects on mycobacterial membranes to defensins, also associates with negatively charged mycobacterial membranes through its positively charged amino acid residues. Consistent with this hypothesis, the sequences between the first and second conserved cysteine residues of the WAP domains are not conserved. Moreover, there are several positively charged amino acids (lysine and arginine) in these regions of the WAP domains that possess antimicrobial activities, whereas the regions without any antimicrobial activities contain one or zero positively charged amino acids. Furthermore, structural studies have revealed that the region between the first and second conserved cysteine residues is exposed on the outside of the molecule, thereby enabling this region to associate with microbial membranes (39, 40). Indeed, mutations of the cationic amino acid residues within this region resulted in elimination of the antimycobacterial activity. Thus, mouse SLPI exhibits antimycobacterial activity in quite a similar manner to that of defensins.

In comparison to SLPI, higher concentrations of other serine protease inhibitors containing a WAP domain are required to inhibit microbial growth (8, 21, 22). Recombinant human SLPI is less effective at inhibiting the growth of mycobacteria and *S. typhimurium* (our unpublished data). These differential properties may be attributable to structural differences in the WAP domains, which mediate the antimicrobial activity. SLPI has two WAP domains, whereas other serine protease inhibitors, such as Eppin, Elafin, and SWAMs, have only a single WAP domain. In the case of human SLPI, only the N-terminal WAP domain exhibits antimicrobial activity (18). In addition, only the N-terminal WAP domain of human SLPI contains critical cationic acid residues. The presence of two WAP domains possessing antimicrobial activity may be responsible for the high potency of mouse SLPI for mycobacterial growth inhibition.

Mouse SLPI inhibited mycobacterial growth at profoundly lower concentrations than those required to inhibit the growth of *S. typhimurium* or other microorganisms (18–20). It remains unclear how SLPI becomes more specifically targeted toward mycobacteria. Differential antimicrobial properties against distinct microorganisms have not been reported in the case of defensins. Therefore, SLPI, which has multifunctional properties, may have an unknown strategy for specifically recognizing mycobacteria.

The in vitro findings demonstrating that mouse SLPI inhibits mycobacterial growth were further strengthened by in vivo studies using $Slpi^{-/-}$ mice. $Slpi^{-/-}$ mice were highly susceptible to pulmonary *M. tuberculosis* infection, but not to i.v. infection. In accordance with this finding, SLPI protein was abundantly detected in the alveolar space after pulmonary BCG infection, but was not detected in sera from mice after i.v. BCG infection (our unpublished data). Therefore, high concentrations of SLPI are supposed to be secreted into the alveolar space during the early phase of respiratory infection with *M. tuberculosis*, thereby promptly killing the mycobacteria before they can invade the lung tissues through the epithelial barrier. Given that mouse SLPI has potent antimycobacterial activities, it would be a good candidate for treatment during the acute phase of *M. tuberculosis* infection and may even be able to be used for the treatment of patients with multidrug-resistant *M. tuberculosis*.

Acknowledgments

We thank S. Ehrt and A. Ding for helpful discussions, Y. Yamada and K. Takeda for technical assistance, and M. Kurata for secretarial assistance.

Disclosures

The authors have no financial conflict of interest.

References

1. Kaufmann, S. H. 2006. Tuberculosis: back on the immunologists' agenda. *Immunity* 24: 351–357.
2. North, R. J., and Y. J. Jung. 2004. Immunity to tuberculosis. *Annu. Rev. Immunol.* 22: 599–623.
3. Fremond, C. M., V. Yeremeev, D. M. Nicolle, M. Jacobs, V. F. Quesniaux, and B. Ryffel. 2004. Fatal *Mycobacterium tuberculosis* infection despite adaptive immune response in the absence of MyD88. *J. Clin. Invest.* 114: 1790–1799.
4. Quesniaux, V., C. Fremond, M. Jacobs, S. Parida, D. Nicolle, V. Yeremeev, F. Bihl, F. Erard, T. Botha, M. Drennan, et al. 2004. Toll-like receptor pathways in the immune responses to mycobacteria. *Microbes Infect.* 6: 946–959.
5. Gerritsen, J. 2000. Host defence mechanisms of the respiratory system. *Paediatr. Respir. Rev.* 1: 128–134.
6. Clauss, A., H. Lilja, and A. Lundwall. 2005. The evolution of a genetic locus encoding small serine proteinase inhibitors. *Biochem. Biophys. Res. Commun.* 333: 383–389.
7. Eisenberg, S. P., K. K. Hale, P. Heimdal, and R. C. Thompson. 1990. Location of the protease-inhibitory region of secretory leukocyte protease inhibitor. *J. Biol. Chem.* 265: 7976–7981.
8. Hagiwara, K., T. Kikuchi, Y. Endo, Huqun, K. Usui, M. Takahashi, N. Shibata, T. Kusakabe, H. Xin, S. Hoshi, et al. 2003. Mouse SWAM1 and SWAM2 are antibacterial proteins composed of a single whey acidic protein motif. *J. Immunol.* 170: 1973–1979.
9. Abe, T., N. Kobayashi, K. Yoshimura, B. C. Trapnell, H. Kim, R. C. Hubbard, M. T. Brewer, R. C. Thompson, and R. G. Crystal. 1991. Expression of the secretory leukoprotease inhibitor gene in epithelial cells. *J. Clin. Invest.* 87: 2207–2215.
10. Hiemstra, P. S., S. van Wetering, and J. Stolk. 1998. Neutrophil serine proteinases and defensins in chronic obstructive pulmonary disease: effects on pulmonary epithelium. *Eur. Respir. J.* 12: 1200–1208.
11. Schiessler, H., E. Fink, and H. Fritz. 1976. Acid-stable proteinase inhibitors from human seminal plasma. *Methods Enzymol.* 45: 847–859.
12. Vogelmeier, C., R. C. Hubbard, G. A. Fells, H. P. Schnebli, R. C. Thompson, H. Fritz, and R. G. Crystal. 1991. Anti-neutrophil elastase defense of the normal human respiratory epithelial surface provided by the secretory leukoprotease inhibitor. *J. Clin. Invest.* 87: 482–488.
13. Wingens, M., B. H. van Bergen, P. S. Hiemstra, J. F. Meis, I. M. van Vlijmen-Willems, P. L. Zeeuwen, J. Mulder, H. A. Kramps, F. van Ruissen, and J. Schalkwijk. 1998. Induction of SLPI (ALP/HUSI-I) in epidermal keratinocytes. *J. Invest. Dermatol.* 111: 996–1002.
14. Gauthier, F., U. Fryksmark, K. Ohlsson, and J. G. Bieth. 1982. Kinetics of the inhibition of leukocyte elastase by the bronchial inhibitor. *Biochim. Biophys. Acta* 700: 178–183.
15. Thompson, R. C., and K. Ohlsson. 1986. Isolation, properties, and complete amino acid sequence of human secretory leukocyte protease inhibitor, a potent inhibitor of leukocyte elastase. *Proc. Natl. Acad. Sci. USA* 83: 6692–6696.
16. Ashcroft, G. S., K. Lei, W. Jin, G. Longenecker, A. B. Kulkarni, T. Greenwell-Wild, H. Hale-Donze, G. McGrady, X. Y. Song, and S. M. Wahl. 2000. Secretory leukocyte protease inhibitor mediates non-redundant functions necessary for normal wound healing. *Nat. Med.* 6: 1147–1153.

17. Zhu, J., C. Nathan, W. Jin, D. Sim, G. S. Ashcroft, S. M. Wahl, L. Lacomis, H. Erdjument-Bromage, P. Tempst, C. D. Wright, and A. Ding. 2002. Conversion of proepithelin to epithelins: roles of SLPI and elastase in host defense and wound repair. *Cell* 111: 867–878.
18. Hiemstra, P. S., R. J. Maassen, J. Stolk, R. Heinzel-Wieland, G. J. Steffens, and J. H. Dijkman. 1996. Antibacterial activity of antileukoprotease. *Infect. Immun.* 64: 4520–4524.
19. McNeely, T. B., D. C. Shugars, M. Rosendahl, C. Tucker, S. P. Eisenberg, and S. M. Wahl. 1997. Inhibition of human immunodeficiency virus type 1 infectivity by secretory leukocyte protease inhibitor occurs prior to viral reverse transcription. *Blood* 90: 1141–1149.
20. Tomee, J. F., P. S. Hiemstra, R. Heinzel-Wieland, and H. F. Kauffman. 1997. Antileukoprotease: an endogenous protein in the innate mucosal defense against fungi. *J. Infect. Dis.* 176: 740–747.
21. Simpson, A. J., A. I. Maxwell, J. R. Govan, C. Haslett, and J. M. Sallenave. 1999. Elafin (elastase-specific inhibitor) has anti-microbial activity against Gram-positive and Gram-negative respiratory pathogens. *FEBS Lett.* 452: 309–313.
22. Yenugu, S., R. T. Richardson, P. Sivashanmugam, Z. Wang, M. G. O'Rand, F. S. French, and S. H. Hall. 2004. Antimicrobial activity of human EPPIN, an androgen-regulated, sperm-bound protein with a whey acidic protein motif. *Biol. Reprod.* 71: 1484–1490.
23. Jin, F. Y., C. Nathan, D. Radzioch, and A. Ding. 1997. Secretory leukocyte protease inhibitor: a macrophage product induced by and antagonistic to bacterial lipopolysaccharide. *Cell* 88: 417–426.
24. Taggart, C. C., S. A. Cryan, S. Weldon, A. Gibbons, C. M. Greene, E. Kelly, T. B. Low, S. J. O'Neill, and N. G. McElvaney. 2005. Secretory leucoprotease inhibitor binds to NF-κB binding sites in monocytes and inhibits p65 binding. *J. Exp. Med.* 202: 1659–1668.
25. Taggart, C. C., C. M. Greene, N. G. McElvaney, and S. O'Neill. 2002. Secretory leucoprotease inhibitor prevents lipopolysaccharide-induced IκBα degradation without affecting phosphorylation or ubiquitination. *J. Biol. Chem.* 277: 33648–33653.
26. Nakamura, A., Y. Mori, K. Hagiwara, T. Suzuki, T. Sakakibara, T. Kikuchi, T. Igarashi, M. Ebina, T. Abe, J. Miyazaki, et al. 2003. Increased susceptibility to LPS-induced endotoxin shock in secretory leukoprotease inhibitor (SLPI)-deficient mice. *J. Exp. Med.* 197: 669–674.
27. Ding, A., H. Yu, J. Yang, S. Shi, and S. Ehrt. 2005. Induction of macrophage-derived SLPI by *Mycobacterium tuberculosis* depends on TLR2 but not MyD88. *Immunology* 116: 381–389.
28. Doi, T., H. Yamada, T. Yajima, W. Wajjwalku, T. Hara, and Y. Yoshikai. 2007. H2-M3-restricted CD8$^+$ T cells induced by peptide-pulsed dendritic cells confer protection against *Mycobacterium tuberculosis*. *J. Immunol.* 178: 3806–3813.
29. deMello, D. E., S. Mahmoud, P. J. Padfield, and J. W. Hoffmann. 2000. Generation of an immortal differentiated lung type-II epithelial cell line from the adult H-2K^{b}tsA58 transgenic mouse. *In Vitro Cell. Dev. Biol. Anim.* 36: 374–382.
30. Aoki, K., S. Matsumoto, Y. Hirayama, T. Wada, Y. Ozeki, M. Niki, P. Domenech, K. Umemori, S. Yamamoto, A. Mineda, et al. 2004. Extracellular mycobacterial DNA-binding protein 1 participates in mycobacterium-lung epithelial cell interaction through hyaluronic acid. *J. Biol. Chem.* 279: 39798–39806.
31. Loh, B., C. Grant, and R. E. Hancock. 1984. Use of the fluorescent probe 1-*N*-phenylnaphthylamine to study the interactions of aminoglycoside antibiotics with the outer membrane of *Pseudomonas aeruginosa*. *Antimicrob. Agents Chemother.* 26: 546–551.
32. Jat, P. S., M. D. Noble, P. Ataliotis, Y. Tanaka, N. Yannoutsos, L. Larsen, and D. Kioussis. 1991. Direct derivation of conditionally immortal cell lines from an H-2K^b-tsA58 transgenic mouse. *Proc. Natl. Acad. Sci. USA* 88: 5096–5100.
33. Whitehead, R. H., P. E. VanEeden, M. D. Noble, P. Ataliotis, and P. S. Jat. 1993. Establishment of conditionally immortalized epithelial cell lines from both colon and small intestine of adult H-2K^b-tsA58 transgenic mice. *Proc. Natl. Acad. Sci. USA* 90: 587–591.
34. Si-Tahar, M., D. Merlin, S. Sitaraman, and J. L. Madara. 2000. Constitutive and regulated secretion of secretory leukocyte proteinase inhibitor by human intestinal epithelial cells. *Gastroenterology* 118: 1061–1071.
35. Kirchhoff, C., I. Habben, R. Ivell, and N. Krull. 1991. A major human epididymis-specific cDNA encodes a protein with sequence homology to extracellular proteinase inhibitors. *Biol. Reprod.* 45: 350–357.
36. Miyakawa, Y., P. Ratnakar, A. G. Rao, M. L. Costello, O. Mathieu-Costello, R. I. Lehrer, and A. Catanzaro. 1996. In vitro activity of the antimicrobial peptides human and rabbit defensins and porcine leukocyte protegrin against *Mycobacterium tuberculosis*. *Infect. Immun.* 64: 926–932.
37. Zasloff, M. 2002. Antimicrobial peptides of multicellular organisms. *Nature* 415: 389–395.
38. Tanabe, H., X. Qu, C. S. Weeks, J. E. Cummings, S. Kolusheva, K. B. Walsh, R. Jelinek, T. K. Vanderlick, M. E. Selsted, and A. J. Ouellette. 2004. Structure-activity determinants in Paneth cell α-defensins: loss-of-function in mouse cryptdin-4 by charge-reversal at arginine residue positions. *J. Biol. Chem.* 279: 11976–11983.
39. Grutter, M. G., G. Fendrich, R. Huber, and W. Bode. 1988. The 2.5 A X-ray crystal structure of the acid-stable proteinase inhibitor from human mucous secretions analysed in its complex with bovine α-chymotrypsin. *EMBO J.* 7: 345–351.
40. Lin, C. C., and J. Y. Chang. 2006. Pathway of oxidative folding of secretory leucocyte protease inhibitor: an 8-disulfide protein exhibits a unique mechanism of folding. *Biochemistry* 45: 6231–6240.

THE JOURNAL OF IMMUNOLOGY

Lipocalin 2-Dependent Inhibition of Mycobacterial Growth in Alveolar Epithelium

Hiroyuki Saiga, Junichi Nishimura, Hirotaka Kuwata, Megumi Okuyama, Sohkichi Matsumoto, Shintaro Sato, Makoto Matsumoto, Shizuo Akira, Yasunobu Yoshikai, Kenya Honda, Masahiro Yamamoto and Kiyoshi Takeda

J Immunol 2008;181;8521-8527

The Journal of Immunology is published twice each month by
The American Association of Immunologists, Inc.,
9650 Rockville Pike, Bethesda, MD 20814-3994.

Print ISSN: 0022-1767 Online ISSN: 1550-6606.

The Journal of Immunology

Lipocalin 2-Dependent Inhibition of Mycobacterial Growth in Alveolar Epithelium[1]

Hiroyuki Saiga,[*,†] Junichi Nishimura,[*] Hirotaka Kuwata,[†] Megumi Okuyama,[*] Sohkichi Matsumoto,[||] Shintaro Sato,[§] Makoto Matsumoto,[†] Shizuo Akira,[§,¶] Yasunobu Yoshikai,[‡] Kenya Honda,[*] Masahiro Yamamoto,[*] and Kiyoshi Takeda[2*,†,¶]

***Mycobacterium tuberculosis* invades alveolar epithelial cells as well as macrophages. However, the role of alveolar epithelial cells in the host defense against *M. tuberculosis* remains unknown. In this study, we report that lipocalin 2 (Lcn2)-dependent inhibition of mycobacterial growth within epithelial cells is required for anti-mycobacterial innate immune responses. Lcn2 is secreted into the alveolar space by alveolar macrophages and epithelial cells during the early phase of respiratory mycobacterial infection. Lcn2 inhibits the in vitro growth of mycobacteria through sequestration of iron uptake. Lcn2-deficient mice are highly susceptible to intratracheal infection with *M. tuberculosis*. Histological analyses at the early phase of mycobacterial infection in Lcn2-deficient mice reveal increased numbers of mycobacteria in epithelial cell layers, but not in macrophages, in the lungs. Increased intracellular mycobacterial growth is observed in alveolar epithelial cells, but not in alveolar macrophages, from Lcn2-deficient mice. The inhibitory action of Lcn2 is blocked by the addition of endocytosis inhibitors, suggesting that internalization of Lcn2 into the epithelial cells is a prerequisite for the inhibition of intracellular mycobacterial growth. Taken together, these findings highlight a pivotal role for alveolar epithelial cells during mycobacterial infection, in which Lcn2 mediates anti-mycobacterial innate immune responses within the epithelial cells. *The Journal of Immunology,* 2008, 181: 8521–8527.**

Tuberculosis is a worldwide disease caused by infection with *Mycobacterium tuberculosis*. Therefore, the host defense mechanisms against *M. tuberculosis* have been intensively investigated, and important roles of T cell-mediated adaptive immunity have been well established (1, 2). In addition, functional characterization of TLRs has recently indicated the importance of innate immunity in the host responses to infection with *M. tuberculosis* (3, 4). In the TLR-mediated anti-mycobacterial immune responses, macrophages and dendritic cells are major effectors that engulf pathogens and produce a variety of proinflammatory mediators. In respiratory mycobacterial infection, alveolar macrophages are the major targets of invasion. However, several evidences indicate that mycobacteria also interact with epithelial cells in the respiratory tract and invade these cells (5–9). Accordingly, epithelial cells in the lungs are expected to play a role during mycobacterial infection by producing antimicrobial mediators (10).

Lipocalin 2 (Lcn2),[3] also known as neutrophil gelatinase-associated lipocalin, siderocalin, 24p3, or uterocalin, a member of the lipocalin family of proteins that bind to small hydrophobic molecules, is produced by epithelial cells and macrophages (11–16). Lcn2 has been shown to mediate several biological processes, including mammary gland involution, induction of apoptosis, and delivery of iron (12, 17–19). In addition, structural studies have demonstrated that Lcn2 binds to enterobactin-type bacterial siderophores, which facilitate iron uptake by bacteria (16). Subsequent studies revealed that Lcn2 also binds to other types of siderophores, such as carboxy-mycobactin (produced by mycobacteria) and bacillibactin (produced by *Bacillus anthracis*) (20, 21). Lcn2 has been shown to interfere with siderophore-mediated iron uptake in *Escherichia coli* (16). Accordingly, mice deficient in Lcn2 are highly susceptible to infection with *E. coli* (22, 23). Thus, Lcn2 mediates the host defense against *E. coli* infection through sequestration of iron, which is essential for the growth and activity of nearly all bacteria (24).

Mycobacteria replicate within cells, especially in the phagosome of macrophages (25), where iron is limited. Outside host cells, free iron is also limited, because almost all iron ions exist as complexes with host proteins with high affinity for iron, such as transferrin and lactoferrin. To overcome the iron deficiency within the host, some species of mycobacteria, such as *M. tuberculosis* and *Mycobacterium bovis* bacillus Calmette-Guérin (BCG), synthesize two type of siderophores, called mycobactin and carboxy-mycobactin (also called exochelin) (26, 27). Mycobactin is hydrophobic, whereas carboxy-mycobactin is hydrophilic. These mycobactins have been shown to remove iron from host iron-binding proteins, such as transferrin and lactoferrin (28). In addition, *M. tuberculosis*

---

*Laboratory of Immune Regulation, Department of Microbiology and Immunology, Graduate School of Medicine, Osaka University, Suita, Osaka, Japan; †Department of Molecular Genetics and ‡Division of Host Defense, Research Center for Prevention of Infectious Diseases, Medical Institute of Bioregulation, Kyushu University, Fukuoka, Japan; §Department of Host Defense, Research Institute for Microbial Diseases and ¶WPI Immunology Frontier Research Center, Osaka University, Suita, Osaka, Japan; and ||Department of Bacteriology, Osaka City University Graduate School of Medicine, Osaka, Japan

Received for publication August 5, 2008. Accepted for publication October 11, 2008.

The costs of publication of this article were defrayed in part by the payment of page charges. This article must therefore be hereby marked *advertisement* in accordance with 18 U.S.C. Section 1734 solely to indicate this fact.

[1] This work was supported by a Grant-in-Aid from the Ministry of Education, Culture, Sports, Science and Technology and the Ministry of Health, Labor and Welfare, as well as the Osaka Foundation for the Promotion of Clinical Immunology.

[2] Address correspondence and reprint requests to Dr. Kiyoshi Takeda, Laboratory of Immune Regulation, Department of Microbiology and Immunology, Graduate School of Medicine, Osaka University, Suita, Osaka, Japan. E-mail address: ktakeda@ongene.med.osaka-u.ac.jp

[3] Abbreviations used in this paper: Lcn2, lipocalin 2; BCG, *Mycobacterium bovis* bacillus Calmette-Guérin; BALF, bronchoalveolar lavage fluid; rLcn2, recombinant Lcn2; SP-C, pro-surfactant protein C; DFO, deferoxamine; AEC, alveolar epithelial cell; CPZ, chlorpromazine.

with mutations in the *mbtB* gene, which lack carboxy-mycobactin and mycobactin, exhibit impaired replication in low-iron medium and within macrophages (27). The mechanisms for the mycobactin-mediated iron acquisition within the phagosome of macrophages have recently been elucidated (29). Because pulmonary epithelial cells are also invaded by mycobacteria, host defense mechanisms that inhibit mycobacterial replication within these cells are expected to exist, however they currently remain unclear.

In the present study, we analyzed the role of Lcn2 in mycobacterial infection. Lcn2, which inhibits mycobacterial growth, was rapidly produced from alveolar macrophages and epithelial cells after mycobacterial infection. Furthermore, analyses using Lcn2-deficient mice revealed a pivotal role of alveolar epithelial cells in mycobacterial infection.

Materials and Methods

Mice

Lcn2$^{-/-}$ and *H-2K*^{b}*-tsA58* transgenic mice have been generated (22, 30) and backcrossed to C57BL/6 for six generations. *Lcn2*$^{-/-}$ and wild-type littermates from intercrosses of *Lcn2*$^{+/-}$ mice were used for experiments at 6–8 wk of age. All animal experiments were conducted in accordance with the guidelines of the Animal Care and Use Committee of Kyushu University and Osaka University.

Mycobacteria

M. bovis BCG (Tokyo strain) was purchased from Kyowa Pharmaceuticals. *M. tuberculosis* strains H37Ra (ATCC25177) and H37Rv (ATCC358121) were grown in Middlebrook 7H9-ADC medium for 2 wk and stored at −80°C until use. GFP-expressing BCG, which was generated previously (5), was used for the experiment.

Quantitative real-time RT-PCR

Total RNA was isolated with the TRIzol reagent (Invitrogen), and reverse transcribed using M-MLV reverse transcriptase (Promega) and random primers (Toyobo) after treatment with RQ1 DNaseI (Promega). Quantitative real-time PCR was performed in ABI7300 (Applied Biosystems) using TaqMan Universal PCR Master Mix (Applied Biosystems). All data are shown as the relative mRNA levels normalized by the corresponding 18S rRNA level. The primers for 18S rRNA and Lcn2 were purchased from Assays on Demand (Applied Biosystems).

Preparation of alveolar macrophages

Bronchoalveolar lavage fluid (BALF) was collected from uninfected mice. To eliminate contamination by bacteria, the cells were cultured with 50 U/ml penicillin and 50 μg/ml streptomycin for 16 h, and then washed five times to remove nonadherent cells. The resultant adherent cells were used for experiments as alveolar macrophages, because >95% of the adherent cells were CD11b-positive.

Preparation of recombinant Lcn2 (rLcn2) protein

A mouse Lcn2 cDNA fragment was inserted into pGEX6P-2 (GE Healthcare) and transformed into *E. coli* BL21. The expressed GST-Lcn2 fusion proteins were purified using glutathione-Sepharose 4B (GE Healthcare) according to the manufacturer's instructions. The purified proteins were incubated with PreScission Protease (GE Healthcare) to cleave the GST tag, and then purified with Glutathione-Sepharose 4B.

Immunohistochemistry

Lungs were fixed with 4% PFA and frozen in Tissue-Tec OCT compound (Sakura). The sections were incubated with anti-mouse Lcn2 Ab (R&D Systems), anti-pro-surfactant protein C (SP-C) Ab (Chemicon), anti-CD11b Ab (BD Biosciences), or anti-pan cytokeratin Ab (Sigma-Aldrich). The nuclei were stained with 4′,6-diamidino-2-phenylindole (DAPI; Molecular Probes). Alveolar epithelial cells were infected with GFP-expressing BCG for 16 h, washed, and incubated with Dextran Conjugates (Cascade Blue; Molecular Probes) and Alexa Fluor 594-labeled rLcn2 for 6 h. rLcn2 was labeled using an Alexa Fluor 594 Protein Labeling Kit (Molecular Probes). The cells were fixed with 4% PFA and analyzed using a confocal microscopy (LSM 510; Carl Zeiss).

Western blot assay

BALF was collected from BCG-infected mice by catheterization techniques into 500 μl of PBS. To normalize BALF samples, we injected the same volume of PBS (500 μl), recovered equal volume, and used them for Western blot analysis. After removal of precipitates, the samples were separated on SDS-PAGE and transferred to PVDF membranes (Millipore). The membranes were incubated with anti-mouse Lcn2 Ab. Bound Ab was detected with SuperSignal West Pico Chemiluminescent Substrate (Pierce).

In vitro mycobacterial growth assay

Mycobacteria were incubated in Middlebrook 7H9-ADC medium with the indicated concentrations of rLcn2 protein for 20 days at 37°C, and were plated on Middlebrook 7H10-OADC agar plates and incubated at 37°C for 30 days. In some experiments, BCG was incubated with the indicated concentrations of deferoxamine mesylate (DFO; Calbiochem), $FeCl_3$ or mycobactin (Kyoritsu Seiyaku) on 7H10-OADC agar plates.

In vivo infection of mycobacteria

Mice were intratracheally infected with *M. tuberculosis* H37Rv (1×10^6 CFU). At 6 wk after infection, homogenates of the lungs and livers were plated on 7H10-OADC agar plates. For histological analyses, the lungs were fixed with 4% PFA at 20 or 5 days after infection, embedded in paraffin, cut into sections, and stained with H&E or by the Ziehl-Neelsen method, respectively.

Establishment of alveolar epithelial cell lines

To establish alveolar epithelial cell lines (AECs) from wild-type and *Lcn2*$^{-/-}$ mice, the mice were crossed with *H-2K*^{b}*-tsA58* transgenic mice, and used for experiments at 4 wk of age. Mouse pulmonary type II AECs were established as previously described (32). The cells were incubated at 33°C and passaged over ten times. The cells were then stained with anti-SP-C Ab to confirm that they were type II alveolar epithelial cells.

In vitro infection of mycobacteria

Wild-type or *Lcn2*$^{-/-}$ derived AECs or alveolar macrophages were incubated with BCG for the indicated periods. To eliminate extracellular BCG, the cells were cultured with 50 μg/ml streptomycin for 1 h, washed three times, and harvested. Lysates of the cells were plated on 7H10-OADC agar plates.

Detection of intracellular growth of mycobacteria

Wild-type and *Lcn2*$^{-/-}$-derived AECs were seeded onto 96-well plates, and infected with BCG for 6 h. To eliminate extracellular BCG, the AECs were cultured with 50 μg/ml streptomycin for 1 h, vigorously washed three times. The cells were pulsed with 37 kBq of [^{3}H]uracil and cultured for 48 h. The cells were harvested on glass fiber filters and the incorporated [^{3}H]uracil was measured using a liquid scintillation counter (Wallac). In some experiments, cytochalasin B (Sigma-Aldrich) or chlorpromazine (CPZ; Calbiochem) was added to the wells at 30 min before the [^{3}H]uracil pulse or rLcn2 addition.

Statistical analysis

Differences between control and experimental groups were evaluated using Student's *t* test or ANOVA plus posthoc testing. Values of $p < 0.05$ were considered to indicate statistical significance.

Results

Expression of lipocalin 2 in BCG-infected lungs

To assess the role of Lcn2 in mycobacterial infection, we first analyzed the expression of Lcn2 in the lungs of C57BL/6 mice intratracheally infected with BCG. Total RNA was extracted from the lungs at 2, 7, and 14 days after infection, and analyzed for Lcn2 mRNA expression by real-time quantitative PCR (Fig. 1*A*). Expression of Lcn2 mRNA was markedly increased at 2 days after infection and decreased thereafter. Because Lcn2 mRNA expression was shown to be induced in macrophages stimulated with TLR ligands (22), we analyzed whether alveolar macrophages expressed Lcn2 mRNA (Fig. 1*B*). Alveolar macrophages were isolated, infected with BCG, and analyzed for Lcn2 mRNA expression at 2 days

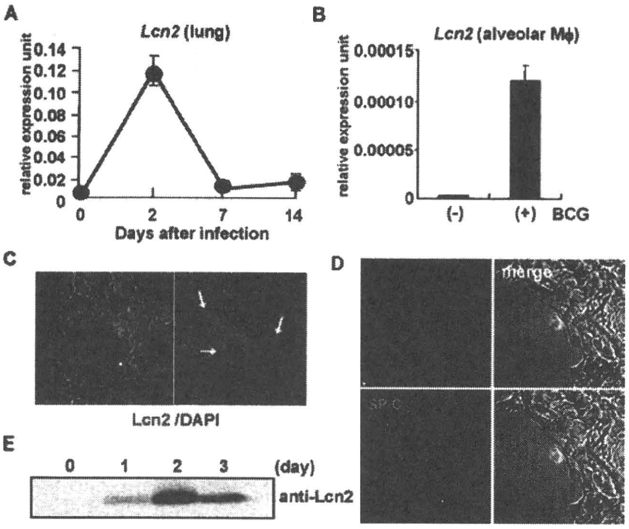

FIGURE 1. Lcn2 expression in the lungs of BCG-infected mice. *A*, Wild-type C57BL/6 mice were intratracheally infected with 2.5 × 10^6 CFU of BCG. Total RNA was extracted from the lungs after the indicated periods. Lcn2 mRNA expression was analyzed by real-time quantitative PCR. Data are shown as the relative mRNA levels normalized by the corresponding 18S rRNA level. Data are presented as means ± SD, and are representative of two independent experiments. *B*, Alveolar macrophages were isolated from uninfected wild-type mice, cultured with or without BCG for 48 h, and then analyzed for their Lcn2 mRNA expression by real-time quantitative PCR. *C* and *D*, At 2 days after intratracheal infection with BCG, lung tissue sections were stained with anti-Lcn2 Ab (red), DAPI (blue), and anti-SP-C Ab (green), and visualized by fluorescence microscopy. *E*, Wild-type mice were intratracheally infected with 2.5 × 10^6 CFU of BCG. At the indicated time points after the infection, 500 μl of PBS was intratracheally injected and then recovered. The recovered BALF samples were subjected to Western blot analysis with anti-Lcn2 Ab.

after infection; BCG infection led to a marked increase in the expression of Lcn2 mRNA. We also analyzed the lungs by immunohistochemistry using an anti BCG-infected mice, several Lcn2-positive cells were observed. These cells mainly faced the alveolar surface and projected into the alveolar space, representing the typical morphology of type II alveolar epithelial cells. Costaining with an Ab to pro-SP-C, which is produced by type II alveolar epithelial cells, revealed that both Lcn2 and SP-C were produced by the same cells (Fig. 1*D*). These findings indicate that not only alveolar macrophages but also type II alveolar epithelial cells produce Lcn2 during respiratory mycobacterial infection. Type II alveolar epithelial cells are known to secrete several mediators into the alveolar space. Therefore, we analyzed whether Lcn2 is secreted into the alveolar space during intratracheal BCG infection. BALF was collected from uninfected and BCG-infected mice and analyzed for Lcn2 protein expression by Western blotting (Fig. 1*E*). Lcn2 was not detected in BALF from uninfected mice. At 2 days after BCG infection, Lcn2 expression was abundantly detected in BALF from the infected mice, indicating that Lcn2 was secreted into the alveolar space during the early phase of mycobacterial infection.

Lcn2-mediated inhibition of mycobacterial growth

We produced rLcn2 and analyzed its effect on in vitro mycobacterial growth. Addition of rLcn2 dose-dependently inhibited the growth of avirulent strains of mycobacteria such as BCG and *M. tuberculosis* H37Ra (Fig. 2, *A* and *B*). rLcn2 also inhibited the growth of virulent *M. tuberculosis* H37Rv in a dose-dependent manner (Fig. 2*C*). Thus, Lcn2 has the ability to inhibit the growth of several mycobacterial strains.

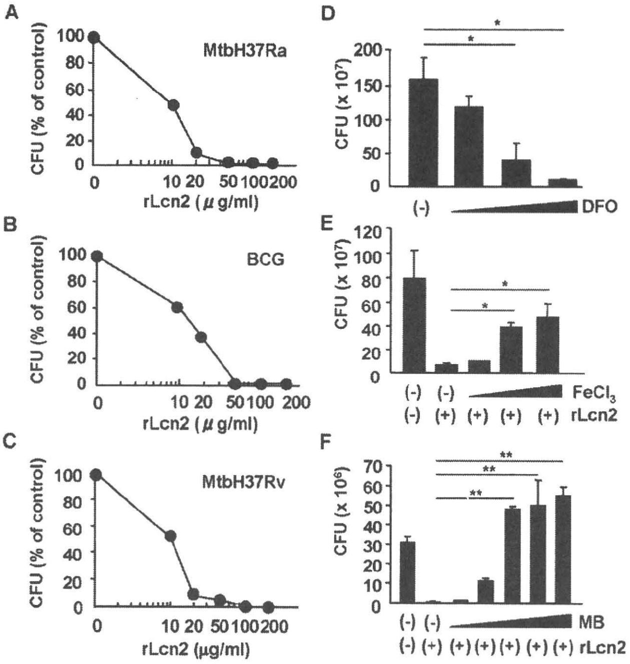

FIGURE 2. Inhibition of in vitro mycobacterial growth by Lcn2. *A–C*, *M. tuberculosis* H37Ra (*A*), BCG (*B*), or *M. tuberculosis* H37Rv (*C*) (1 × 10^6 CFU each) was incubated with the indicated concentrations of rLcn2 in 7H9 ADC medium for 20 days and then plated on 7H10-OADC agar. The CFU numbers were counted. *D*, BCG was incubated with increasing concentrations of DFO (1 μM, 100 μM and 1 mM) for 20 days and then plated on 7H10-OADC agar. The CFU numbers were counted. *E* and *F*, BCG was incubated in the presence of rLcn2 (50 μg/ml) as well as increasing concentrations of $FeCl_3$ (*E*: 5 nM, 500 nM, 50 μM, and 5 mM) or MB (*F*: 1 pg/ml, 10 pg/ml, 1 ng/ml, 100 ng/ml, and 10 μg/ml) (*F*) for 20 days, and then plated on 7H10-OADC agar. All data are presented as means ± SD. * and ** indicate a significant difference among groups, ANOVA, posthoc Scheffe; *, $p < 0.05$; **, $p < 0.005$.

We investigated whether Lcn2 inhibits mycobacterial growth by interfering with iron acquisition, similar to the case for inhibition of *E. coli* growth (16). First, we added DFO, an iron chelator, into in vitro BCG cultures (Fig. 2*D*). DFO reduced BCG growth in a dose-dependent manner, indicating that BCG requires iron for growth. Next, we added ferric iron into BCG cultures (Fig. 2*E*). Addition of ferric iron rescued Lcn2-mediated inhibition of BCG growth in a dose-dependent manner, indicating that Lcn2 inhibits use of iron from the culture medium. Addition of exogenous mycobactin (MB) also abolished Lcn2-mediated inhibition of BCG growth (Fig. 2*F*). These findings indicate that Lcn2 inhibits mycobacterial growth by sequestering iron.

In vivo anti-mycobacterial activity of lipocalin 2

We next addressed the in vivo role of Lcn2 in *M. tuberculosis* infection using *Lcn2*$^{-/-}$ mice. Wild-type and *Lcn2*$^{-/-}$ mice were intratracheally infected with *M. tuberculosis* H37Rv and monitored for their survival (Fig. 3*A*). *Lcn2*$^{-/-}$ mice were highly sensitive to intratracheal infection with *M. tuberculosis* and many of the infected mice died. We also counted the CFU numbers in the lungs and livers after 6 wk of infection (Fig. 3*B*). The CFU titer of *M. tuberculosis* was higher in *Lcn2*$^{-/-}$ mice than that in wild-type mice. Histopathological analysis of the lungs of the infected mice at 20 days after infection revealed that the number and size of the granulomatous lesions were increased in *Lcn2*$^{-/-}$ mice (Fig. 3*C*), indicating that the inflammatory response in *Lcn2*$^{-/-}$ mice was enhanced, possibly due to progression of the *M. tuberculosis* infection. These findings demonstrate that Lcn2 plays an important role in host resistance to *M. tuberculosis* infection in vivo.

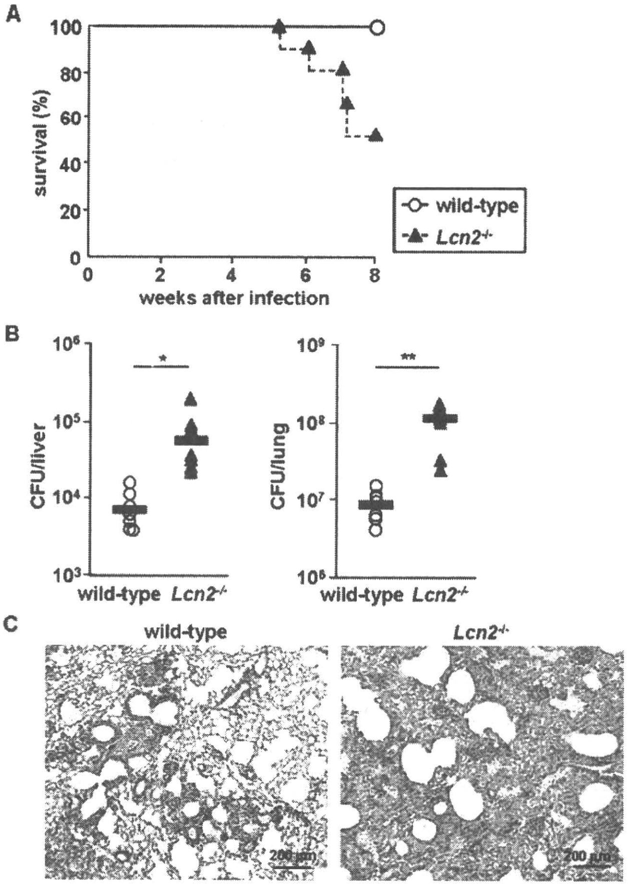

FIGURE 3. High susceptibility of *Lcn2*$^{-/-}$ mice to *M. tuberculosis* infection. *A*, Wild-type (n = 11) and *Lcn2*$^{-/-}$ (n = 12) mice were intratracheally infected with *M. tuberculosis* H37Rv (1 × 10^6 CFU) and their survival was monitored for 8 wk. *B*, Wild-type (n = 7) and *Lcn2*$^{-/-}$ (n = 7) mice were intratracheally infected with *M. tuberculosis* H37Rv (1 × 10^6 CFU). At 6 wk after infection, homogenates of the lungs and livers were plated on 7H10-OADC agar and the CFU titers were counted. Symbols represent individual mice, and bars represent the mean CFU numbers. *, $p < 0.05$; **, $p < 0.005$. Data are representative of two independent experiments. *C*, H&E staining of representative lung tissues from wild-type and *Lcn2*$^{-/-}$ mice at 20 days after intratracheal infection with *M. tuberculosis*.

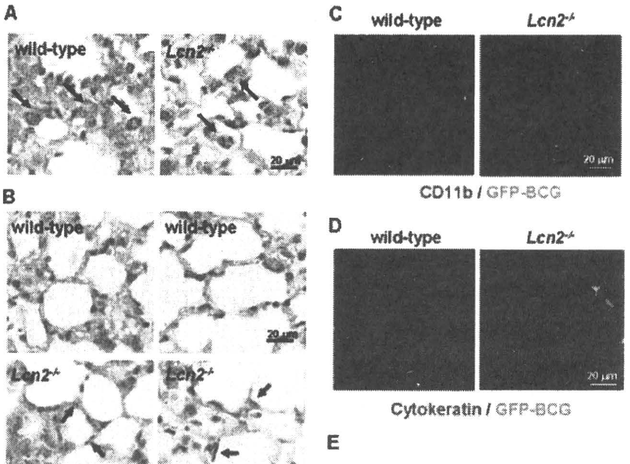

E

Number of cells that are invaded with BCG

	cytokeratin positive cells	cytokeratin negative cells	total
Wild-type	25 (37%)	42 (63%)	67
Lcn2-/-	104 (73%)	37 (27%)	141

FIGURE 4. Increased numbers of *M. tuberculosis* in *Lcn2*$^{-/-}$ alveolar epithelial cells. *A* and *B*, Wild-type and *Lcn2*$^{-/-}$ mice were intratracheally infected with *M. tuberculosis* H37Ra. At 5 days after infection, the lungs were fixed in paraffin, sectioned, and stained with the Ziehl-Neelsen method. Arrows indicate red-stained *M. tuberculosis*. *C–E*, At 5 days after intratracheal infection with GFP-expressing BCG (green), lung tissue sections were stained with anti-CD11b Ab (*C*, red) or anti-pan-cytokeratin Ab (*D*, red), and visualized by fluorescence microscopy. The number of cells containing BCG was counted in a total of ten areas of pictures that visualized different fields (*E*).

Increased numbers of mycobacteria in Lcn2-deficient alveolar epithelial cells

We next analyzed the localization of *M. tuberculosis* in the lungs at 5 days after intratracheal infection by staining acid-fast bacilli using the Ziehl-Neelsen method. In wild-type and *Lcn2*$^{-/-}$ mice, similar densities of *M. tuberculosis* were observed in granulomatous lesions, although the number and size of the granulomatous lesions were increased in *Lcn2*$^{-/-}$ mice (data not shown). In addition, *M. tuberculosis* exhibited similar staining of cells with a macrophage-like morphology in wild-type and *Lcn2*$^{-/-}$ mice (Fig. 4*A*). Strikingly, some of the alveolar epithelial cell layers in *Lcn2*$^{-/-}$ mice contained *M. tuberculosis* (Fig. 4*B*). In sharp contrast, *M. tuberculosis* was scarcely detected within the epithelial cell layers of wild-type mice. To corroborate these findings, we subjected the lungs of mice intratracheally infected with GFP-expressing BCG to immunohistochemical analyses. In both wild-type and *Lcn2*$^{-/-}$ mice, CD11b-positive cells contained GFP-expressing BCG. However, in the lungs of *Lcn2*$^{-/-}$ mice, GFP-expressing BCG was frequently observed in cells that did not express CD11b, in contrast to the low frequency observed in the lungs of wild-type mice (Fig. 4*C*). Visualization of epithelial cells using an anti-cytokeratin Ab indicated that increased numbers of alveolar epithelial cells in *Lcn2*$^{-/-}$ mice contained GFP-expressing BCG compared with those in wild-type mice (Fig. 4, *D* and *E*). Thus, in the absence of Lcn2, invasion and replication of mycobacteria in alveolar epithelial cells were increased.

Therefore, we assessed the sensitivities of alveolar macrophages and alveolar epithelial cells to in vitro infection with BCG. First, alveolar macrophages were isolated from wild-type and *Lcn2*$^{-/-}$ mice, and infected with BCG (Fig. 5*A*). The CFU titers of BCG in macrophages at 4 and 7 days after infection were comparable between wild-type and *Lcn2*$^{-/-}$ cells. Thus, the absence of Lcn2 did not affect the anti-mycobacterial activity in alveolar macrophages. Next, we established AECs from wild-type and *Lcn2*$^{-/-}$ mice. Because AECs are difficult to culture in vitro, we took advantage of transgenic mice harboring a temperature-sensitive mutation of the SV40 large tumor Ag gene under the control of an IFN-γ-inducible H-2K^b promoter element (30–32). Using these mice, we successfully established wild-type and *Lcn2*$^{-/-}$ AECs, both of which were stained with anti-SP-C Ab (data not shown). AECs from wild-type mice expressed Lcn2 mRNA and secreted Lcn2 protein into the culture medium when infected with BCG (data not shown). Thus, these AECs showed the characteristics of type II alveolar epithelial cells. AECs were infected with BCG, and the CFU titers within the cells were counted at 1, 2, 3, and 4 days after infection (Fig. 5*B*). At 3 and 4 days after infection, the CFU titers in *Lcn2*$^{-/-}$ cells were increased compared with those in wild-type cells. Addition of exogenous rLcn2 reduced the CFU numbers in *Lcn2*$^{-/-}$ cells (Fig. 5*C*). Taken together, these findings indicate that the high susceptibility of *Lcn2*$^{-/-}$ mice to *M. tuberculosis* infection is attributable to impaired clearance of mycobacteria from alveolar epithelial cells, rather than alveolar macrophages, in the absence of Lcn2.

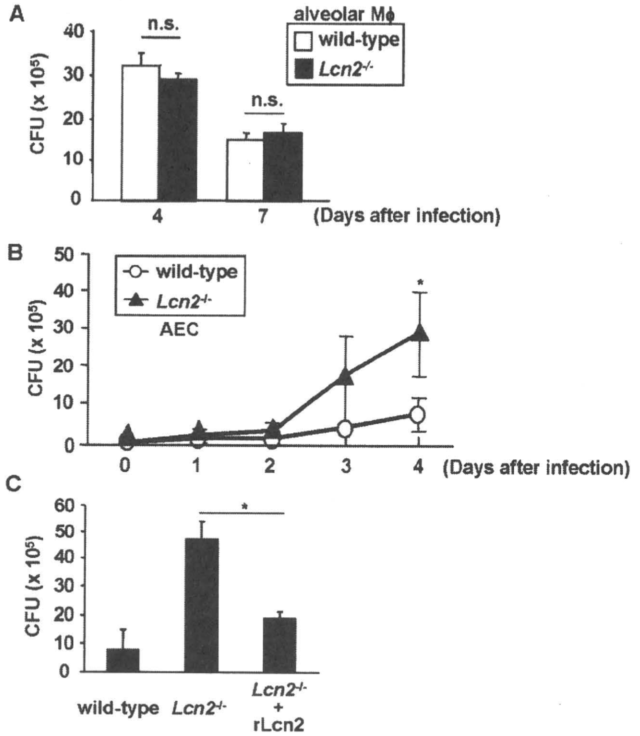

FIGURE 5. Increased BCG growth in *Lcn2*$^{-/-}$ alveolar epithelial cells. *A*, Alveolar macrophages were collected from uninfected wild-type and *Lcn2*$^{-/-}$ mice and cultured with BCG for the indicated periods. To eliminate external BCG, the cells were cultured with streptomycin for 1 h, washed three times, and harvested. Lysates of the cells were plated on 7H10-OADC agar, and the CFU numbers were counted. Representative data of two independent experiments are shown. n.s., not significant. *B*, Wild-type and *Lcn2*$^{-/-}$ AECs were cultured with BCG for the indicated periods. After removal of extracellular BCG, lysates the cells were plated on 7H10-OADC agar, and the CFU numbers were counted. Data are presented as means ± SD of triplicate determinations and are representative of three independent experiments. $*$, $p < 0.05$. Similar results were obtained when other AECs from wild-type and *Lcn2*$^{-/-}$ mice were used. *C*, Wild-type and *Lcn2*$^{-/-}$ AECs were cultured with BCG. At 2 days after infection, rLcn2 (final concentration 30 μg/ml) was added to the *Lcn2*$^{-/-}$ AEC. After an additional 2 days of culture, the cells were incubated with streptomycin for 1 h, washed three times, and harvested. Lysates of the cells were plated on 7H10-OADC agar, and the CFU numbers were counted. Representative data of three independent experiments are shown. Data are presented as means ± SD of triplicate determinations. $*$, $p < 0.05$.

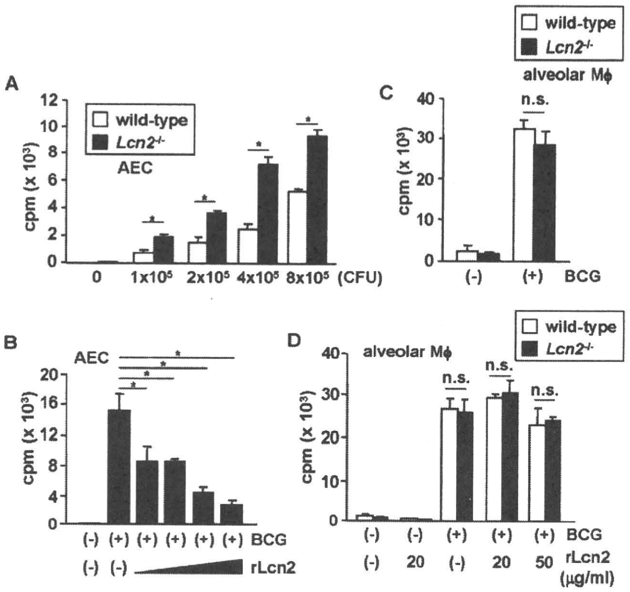

FIGURE 6. Lcn2-mediated inhibition of intracellular BCG growth. *A*, Wild-type and *Lcn2*$^{-/-}$ AECs were seeded onto 96-well plates and infected with the indicated CFUs of BCG for 6 h. The cells were then extensively washed to remove extracellular BCG and cultured in the presence of [^{3}H]uracil for 48 h. The incorporation of [^{3}H]uracil was measured. Data are presented as means ± SD of triplicate samples. Representative data of three independent experiments are shown. $*$, $p < 0.005$. *B*, *Lcn2*$^{-/-}$ AECs were seeded onto 96-well plates, and infected with BCG (2×10^5 CFU) for 6 h. After vigorous washing, the cells were cultured with increasing concentrations of rLcn2 (20, 30, 40, and 50 μg/ml) and [^{3}H]uracil for 48 h, before being measured for their [^{3}H]uracil incorporation. Data are presented as means ± SD of triplicate samples, and are representative of two independent experiments. $*$ indicate a significant difference among groups, ANOVA, posthoc Scheffe, $*$, $p < 0.001$. *C*, Alveolar macrophages were collected from uninfected wild-type and *Lcn2*$^{-/-}$ mice, and cultured with BCG for 6 h. After vigorous washing, the cells were cultured in the presence of [^{3}H]uracil for 48 h, before being measured for their [^{3}H]uracil incorporation. Data are presented as the mean ± SD of triplicate samples. n.s., not significant. *D*, Alveolar macrophages from wild-type and *Lcn2*$^{-/-}$ mice were infected with BCG for 6 h. After vigorous washing, the cells were cultured in the presence of the indicated concentration of rLcn2 and [^{3}H]uracil for 48 h. Then, the [^{3}H]uracil incorporation was counted. Data are presented as means ± SD of triplicate samples. n.s., not significant.

Inhibition of intracellular mycobacterial growth by Lcn2

Mycobacteria are intracellular bacteria that replicate within cells. In the experiments performed so far, it is possible that extracellular growth was monitored as well as intracellular growth under the in vitro conditions. Therefore, to assess the intracellular growth of mycobacteria more precisely, we used [^{3}H]uracil, which is preferentially incorporated into mycobacterial nucleic acids (33). AECs derived from wild-type and *Lcn2*$^{-/-}$ mice were infected with several CFUs of BCG for 6 h, extensively washed with culture medium containing streptomycin to exclude extracellular BCG, and then cultured for 2 days in the presence of [^{3}H]uracil (Fig. 6*A*). Under these conditions, [^{3}H]uracil incorporation was below 1×10^2 cpm in wells containing uninfected AECs or wells placed in contact with BCG and then extensively washed. After infection with each CFU, [^{3}H]uracil incorporation was increased in *Lcn2*$^{-/-}$ cells compared with wild-type cells. In BCG-infected *Lcn2*$^{-/-}$ cells, addition of exogenous rLcn2 reduced the uptake of [^{3}H]uracil by intracellular BCG (Fig. 6*B*). In alveolar macrophages, the [^{3}H]uracil incorporation by intracellular BCG was comparable between wild-type and *Lcn2*$^{-/-}$ cells (Fig. 6*C*). Addition of rLcn2 did not effectively reduce the uptake of [^{3}H]uracil by intracellular BCG in alveolar macrophages from both wild-type and *Lcn2*$^{-/-}$ mice (Fig. 6*D*). These findings indicate that extracellular Lcn2 limits intracellular growth of BCG in AECs, but not in alveolar macrophages.

Because extracellular Lcn2 modulated intracellular mycobacterial growth in the AECs, we analyzed whether extracellular Lcn2 was incorporated into the AECs as described in several previous reports (18, 19). AECs were infected with GFP-expressing BCG and then treated with fluorescein-labeled rLcn2 (Fig. 7*A*). Lcn2 was detected within the AECs, and colocalized with dextran that was taken up into the cells by endocytosis. Furthermore, many BCG were colocalized with rLcn2, indicating that endocytosed Lcn2 was in close proximity to intracellular BCG. In contrast, although Lcn2 was incorporated into alveolar macrophages, the incorporated Lcn2 was not colocalized with BCG in alveolar macrophages (Fig. 7*B*), indicating that BCG and rLcn2 were localized in distinct cellular compartments within macrophages. We blocked

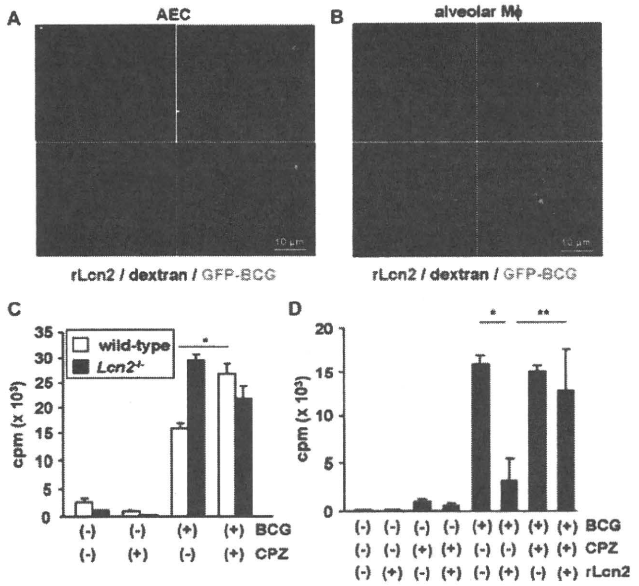

FIGURE 7. Requirement of Lcn2 incorporation for the inhibition of intracellular BCG growth. *A*, GFP-expressing BCG (green)-infected alveolar epithelial cells were cultured with dextran (25 μg/ml; blue) and fluorescein-labeled rLcn2 (15 μg/ml; red) for 6 h. The cells were then washed, fixed with 4% PFA, and analyzed by confocal microscopy. Data are representative of three independent experiments. *B*, GFP-expressing BCG (green)-infected alveolar macrophages were cultured with dextran (25 μg/ml; blue) and fluorescein-labeled rLcn2 (15 μg/ml; red) for 6 h. The cells were then washed, fixed with 4% PFA for 5 min, and analyzed by confocal microscopy. *C*, Wild-type and $Lcn2^{-/-}$ AECs were seeded onto 96-well plates and infected with BCG (2 × 10^5 CFU) for 6 h. After extensive washing, the cells were cultured with CPZ (10 μM) and [^{3}H]uracil for 48 h. The [^{3}H]uracil incorporation was then measured. Data are presented as means ± SD of triplicate samples, and are representative of two independent experiments. *, $p < 0.01$. *D*, $Lcn2^{-/-}$ AECs were seeded onto 96-well plates, and infected with BCG for 6 h. After washing, the cells were cultured with CPZ for 30 min and then cultured with rLcn2 (20 μg/ml) and [^{3}H]uracil for 48 h. The [^{3}H]uracil incorporation was measured. Data are presented as means ± SD of triplicate samples, and are representative of two independent experiments. * or ** indicate a significant difference among groups, ANOVA, posthoc Scheffe, *, $p < 0.005$; **, $p < 0.05$.

endocytosis of Lcn2 using CPZ after BCG infection. Addition of CPZ resulted in increased BCG growth in wild-type AECs, but not in $Lcn2^{-/-}$ cells (Fig. 7*C*). We also analyzed the effects of the endocytosis inhibitor on rLcn2-mediated inhibition of BCG growth (Fig. 7*D*). Addition of CPZ abolished Lcn2-mediated inhibition of [^{3}H]uracil incorporation in both wild-type and $Lcn2^{-/-}$ cells. Cytochalasin B, which also blocks endocytosis, had similar effects to those of CPZ on Lcn2-mediated inhibition of intracellular BCG growth (data not shown). These findings indicate that endocytosed Lcn2 inhibits the intracellular growth of BCG in AECs.

Discussion

Lcn2 has a variety of putative functions, as evident from its many different names such as neutrophil gelatinase-associated lipocalin, uterocalin, 24p3, and siderocalin (12, 13, 16, 19). In the context of its function in host defense, a structural study of the Lcn2 protein revealed that it associates with enterobactin-type bacterial siderophores (16). Subsequently, Lcn2 was shown to bind to several types of siderophores such as caroboxy-mycobactin and bacillibactin (20, 21). In addition, Lcn2 has been proposed to bind to an as-yet unknown mammalian siderophore (18, 34). Thus, Lcn2 has the ability to bind to a variety of types of siderophores. Furthermore, Lcn2 has been shown to inhibit the growth of *E. coli* through sequestration of iron uptake (22, 23). The present study has demonstrated that Lcn2 also participates in the inhibition of mycobacterial growth through similar mechanisms to those against *E. coli*. Indeed, Lcn2 has been shown to associate with the mycobacteria-derived hydrophilic siderophore carboxy-mycobactin (21). In accordance with our results, Lcn2 has been shown to be secreted from neutrophils during *M. tuberculosis* infection and inhibit their growth (35). Lcn2 was originally identified as a molecule that is secreted from neutrophils, which are rapidly recruited to *M. tuberculosis*-infected lungs. Therefore, neutrophils are presumably the source of Lcn2 as well as alveolar macrophages and epithelial cell during *M. tuberculosis* infection.

Regarding the high sensitivity of $Lcn2^{-/-}$ mice to *M. tuberculosis* infection, it is noteworthy that $Lcn2^{-/-}$ alveolar epithelial cells, but not macrophages, contained increased numbers of *M. tuberculosis* at the early phase of the infection, as evaluated by histopathological and immunohistochemical analyses. This finding was unexpected, because successful in vivo detection of mycobacteria in respiratory epithelial cells in wild-type mice has only been achieved through analyses of mycobacterial DNA or use of electron microscopy, even though mycobacteria have been shown to invade epithelial cells as well as macrophages in vitro (6–9, 36). In addition, $Lcn2^{-/-}$ alveolar epithelial cells, but not macrophages, exhibited defective inhibition of intracellular mycobacterial growth, suggesting that impaired inhibition of mycobacterial growth in alveolar epithelial cells due to the absence of Lcn2 may be a major cause of the high susceptibility $Lcn2^{-/-}$ mice to *M. tuberculosis* infection. Given that mycobacteria were easily detected in the alveolar epithelial cell layers by a typical histological approach in the absence of Lcn2 and the increased mycobacterial growth was observed in $Lcn2^{-/-}$ epithelial cells, but not in macrophages, epithelial cells may play an important role in the host immune responses against respiratory infection with *M. tuberculosis*.

Mycobacteria replicate within cells in vivo, and several lines of evidence indicate that mycobactin-mediated iron uptake is a prerequisite for intracellular mycobacterial growth (27, 29). Consistent with previous studies (18, 19), our findings indicated that Lcn2 is internalized into alveolar epithelial cells via endocytosis. Furthermore, addition of rLcn2 effectively inhibited intracellular mycobacterial growth in AECs, and this effect was abolished by endocytosis inhibitors. At present, it remains unclear how mycobacteria take up iron within epithelial cells using mycobactin. First, it is apparent that mycobacteria exist in the phagosome of macrophages. However, the subcellular localization of mycobacteria within epithelial cells has not been established, although mycobacteria have been shown to be localized in endosomes or macropinosomes (37, 38). Our results revealed colocalization of mycobacteria and dextran, indicating that mycobacteria exist in the endosome-like vacuole within epithelial cells. Second, it remains obscure whether mycobacteria secrete water-soluble carboxy-mycobactin into the cytoplasm to bind the cytosolic iron. It is also obscure how endocytosed Lcn2 approaches the carboxy-mycobactin/iron complexes within the cells. Given that Lcn2 and mycobacteria are colocalized within the endosome-like structure, it is possible that mycobacteria take up the iron entering the endosome using mycobactin, and endocytosed Lcn2, in turn, binds to the carboxy-mycobactin/iron complexes, thereby blocking iron acquisition by mycobacteria. Further studies are required to clarify the precise mechanisms for the interaction between Lcn2 and mycobacteria-derived carboxy-mycobactin.

In alveolar macrophages, the absence of Lcn2 did not affect the sensitivity to mycobacterial infection. This may be due to the differential localizations of mycobacteria in epithelial cells and macrophages. Lcn2 was colocalized with mycobacteria in epithelial cells, indicating that mycobacteria exist within the endosome-like structure. In contrast, mycobacteria were localized within the phagosome in macrophages, leading to distinct localizations of Lcn2 and mycobacteria in macrophages. Alternatively, macrophages are professional cells that kill intracellular bacteria by producing several macrophage-specific anti-microbial mediators, including NO synthase and Nramp1 (39–41). These mediators may compensate the Lcn2 deficiency in macrophages. In contrast, they are not expressed in epithelial cells, resulting in the high sensitivity to mycobacterial infection in the absence of Lcn2. Thus, in alveolar epithelial cells, Lcn2 may be a major factor that mediates host resistance to mycobacterial infection.

Our results highlight a novel innate host defense system that inhibits mycobacterial infection at the respiratory mucosal surface. We would like to propose the following scenario with regard to the function of Lcn2. Lcn2 is secreted into the alveolar space by alveolar macrophages and epithelial cells during the early phase of respiratory mycobacterial infection. Lcn2 presumably inhibits mycobacterial growth within the alveolar space. In addition, Lcn2 is internalized into the alveolar epithelial cells, which are invaded by mycobacteria, and inhibits mycobacterial growth by sequestering iron uptake. This leads to a reduction in the number of infected mycobacteria at the early phase of infection, which may help to create sufficient time for effective activation of anti-mycobacterial innate and adaptive immune responses. Thus, respiratory epithelial cells play an active role in the resistance to mycobacterial infection, in addition to their functions as physical barriers and secretors of anti-bacterial mediators.

Acknowledgments

We thank I. Sugawara for providing the *M. tuberculosis* H37Rv, Y. Yamada and K. Takeda for technical assistance, and M. Kurata and M. Yasuda for secretarial assistance.

Disclosures

The authors have no financial conflict of interest.

References

1. North, R. J., and Y. J. Jung. 2004. Immunity to tuberculosis. *Annu. Rev. Immunol.* 22: 599–623.
2. Kaufmann, S. H. 2006. Tuberculosis: back on the immunologists' agenda. *Immunity* 24: 351–357.
3. Quesniaux, V., C. Fremond, M. Jacobs, S. Parida, D. Nicolle, V. Yeremeev, F. Bihl, F. Erard, T. Botha, M. Drennan, et al. 2004. Toll-like receptor pathways in the immune responses to mycobacteria. *Microbes Infect.* 6: 946–959.
4. Fremond, C. M., V. Yeremeev, D. M. Nicolle, M. Jacobs, V. F. Quesniaux, and B. Ryffel. 2004. Fatal *Mycobacterium tuberculosis* infection despite adaptive immune response in the absence of MyD88. *J. Clin. Invest.* 114: 1790–1799.
5. Aoki, K., S. Matsumoto, Y. Hirayama, T. Wada, Y. Ozeki, M. Niki, P. Domenech, K. Umemori, S. Yamamoto, A. Mineda, et al. 2004. Extracellular mycobacterial DNA-binding protein 1 participates in mycobacterium-lung epithelial cell interaction through hyaluronic acid. *J. Biol. Chem.* 279: 39798–39806.
6. Teitelbaum, R., W. Schubert, L. Gunther, Y. Kress, F. Macaluso, J. W. Pollard, D. N. McMurray, and B. R. Bloom. 1999. The M cell as a portal of entry to the lung for the bacterial pathogen *Mycobacterium tuberculosis*. *Immunity* 10: 641–651.
7. Bermudez, L. E., and F. J. Sangari. 2001. Cellular and molecular mechanisms of internalization of mycobacteria by host cells. *Microbes Infect.* 3: 37–42.
8. Bermudez, L. E., F. J. Sangari, P. Kolonoski, M. Petrofsky, and J. Goodman. 2002. The efficiency of the translocation of *Mycobacterium tuberculosis* across a bilayer of epithelial and endothelial cells as a model of the alveolar wall is a consequence of transport within mononuclear phagocytes and invasion of alveolar epithelial cells. *Infect. Immun.* 70: 140–146.
9. Hernandez-Pando, R., M. Jeyanathan, G. Mengistu, D. Aguilar, H. Orozco, M. Harboe, G. A. Rook, and G. Bjune. 2000. Persistence of DNA from *Mycobacterium tuberculosis* in superficially normal lung tissue during latent infection. *Lancet* 356: 2133–2138.
10. Ferguson, J. S., and L. S. Schlesinger. 2000. Pulmonary surfactant in innate immunity and the pathogenesis of tuberculosis. *Tuber. Lung Dis.* 80: 173–184.
11. Kjeldsen, L., J. B. Cowland, and N. Borregaard. 2000. Human neutrophil gelatinase-associated lipocalin and homologous proteins in rat and mouse. *Biochim. Biophys. Acta* 1482: 272–283.
12. Devireddy, L. R., J. G. Teodoro, F. A. Richard, and M. R. Green. 2001. Induction of apoptosis by a secreted lipocalin that is transcriptionally regulated by IL-3 deprivation. *Science* 293: 829–834.
13. Kjeldsen, L., A. H. Johnsen, H. Sengelov, and N. Borregaard. 1993. Isolation and primary structure of NGAL, a novel protein associated with human neutrophil gelatinase. *J. Biol. Chem.* 268: 10425–10432.
14. Flower, D. R., A. C. North, and T. K. Attwood. 1991. Mouse oncogene protein 24p3 is a member of the lipocalin protein family. *Biochem. Biophys. Res. Commun.* 180: 69–74.
15. Liu, Q., J. Ryon, and M. Nilsen-Hamilton. 1997. Uterocalin: a mouse acute phase protein expressed in the uterus around birth. *Mol. Reprod. Dev.* 46: 507–514.
16. Goetz, D. H., M. A. Holmes, N. Borregaard, M. E. Bluhm, K. N. Raymond, and R. K. Strong. 2002. The neutrophil lipocalin NGAL is a bacteriostatic agent that interferes with siderophore-mediated iron acquisition. *Mol. Cell* 10: 1033–1043.
17. Nilsen-Hamilton, M., Q. Liu, J. Ryon, L. Bendickson, P. Lepont, and Q. Chang. 2003. Tissue involution and the acute phase response. *Ann. NY Acad. Sci.* 995: 94–108.
18. Devireddy, L. R., C. Gazin, X. Zhu, and M. R. Green. 2005. A cell-surface receptor for lipocalin 24p3 selectively mediates apoptosis and iron uptake. *Cell* 123: 1293–1305.
19. Yang, J., D. Goetz, J. Y. Li, W. Wang, K. Mori, D. Setlik, T. Du, H. Erdjument-Bromage, P. Tempst, R. Strong, and J. Barasch. 2002. An iron delivery pathway mediated by a lipocalin. *Mol. Cell* 10: 1045–1056.
20. Abergel, R. J., M. K. Wilson, J. E. Arceneaux, T. M. Hoette, R. K. Strong, B. R. Byers, and K. N. Raymond. 2006. Anthrax pathogen evades the mammalian immune system through stealth siderophore production. *Proc. Natl. Acad. Sci. USA* 103: 18499–18503.
21. Holmes, M. A., W. Paulsene, X. Jide, C. Ratledge, and R. K. Strong. 2005. Siderocalin (Lcn 2) also binds carboxymycobactins, potentially defending against mycobacterial infections through iron sequestration. *Structure* 13: 29–41.
22. Flo, T. H., K. D. Smith, S. Sato, D. J. Rodriguez, M. A. Holmes, R. K. Strong, S. Akira, and A. Aderem. 2004. Lipocalin 2 mediates an innate immune response to bacterial infection by sequestrating iron. *Nature* 432: 917–921.
23. Berger, T., A. Togawa, G. S. Duncan, A. J. Elia, A. You-Ten, A. Wakeham, H. E. Fong, C. C. Cheung, and T. W. Mak. 2006. Lipocalin 2-deficient mice exhibit increased sensitivity to *Escherichia coli* infection but not to ischemia-reperfusion injury. *Proc. Natl. Acad. Sci. USA* 103: 1834–1839.
24. Smith, K. D. 2007. Iron metabolism at the host pathogen interface: lipocalin 2 and the pathogen-associated iroA gene cluster. *Int. J. Biochem. Cell Biol.* 39: 1776–1780.
25. Houben, E. N., L. Nguyen, and J. Pieters. 2006. Interaction of pathogenic mycobacteria with the host immune system. *Curr. Opin. Microbiol.* 9: 76–85.
26. De Voss, J. J., K. Rutter, B. G. Schroeder, and C. E. Barry, 3rd. 1999. Iron acquisition and metabolism by mycobacteria. *J. Bacteriol.* 181: 4443–4451.
27. De Voss, J. J., K. Rutter, B. G. Schroeder, H. Su, Y. Zhu, and C. E. Barry, 3rd. 2000. The salicylate-derived mycobactin siderophores of *Mycobacterium tuberculosis* are essential for growth in macrophages. *Proc. Natl. Acad. Sci. USA* 97: 1252–1257.
28. Gobin, J., and M. A. Horwitz. 1996. Exochelins of *Mycobacterium tuberculosis* remove iron from human iron-binding proteins and donate iron to mycobactins in the *M. tuberculosis* cell wall. *J. Exp. Med.* 183: 1527–1532.
29. Luo, M., E. A. Fadeev, and J. T. Groves. 2005. Mycobactin-mediated iron acquisition within macrophages. *Nat. Chem. Biol.* 1: 149–153.
30. Jat, P. S., M. D. Noble, P. Ataliotis, Y. Tanaka, N. Yannoutsos, L. Larsen, and D. Kioussis. 1991. Direct derivation of conditionally immortal cell lines from an H-2Kb-tsA58 transgenic mouse. *Proc. Natl. Acad. Sci. USA* 88: 5096–5100.
31. Whitehead, R. H., P. E. VanEeden, M. D. Noble, P. Ataliotis, and P. S. Jat. 1993. Establishment of conditionally immortalized epithelial cell lines from both colon and small intestine of adult H-2Kb-tsA58 transgenic mice. *Proc. Natl. Acad. Sci. USA* 90: 587–591.
32. deMello, D. E., S. Mahmoud, P. J. Padfield, and J. W. Hoffmann. 2000. Generation of an immortal differentiated lung type-II epithelial cell line from the adult H-2K(b)tsA58 transgenic mouse. *In Vitro Cell. Dev. Biol. Anim.* 36: 374–382.
33. Rook, G. A., B. R. Champion, J. Steele, A. M. Varey, and J. L. Stanford. 1985. I-A restricted activation by T cell lines of anti-tuberculosis activity in murine macrophages. *Clin. Exp. Immunol.* 59: 414–420.
34. Mori, K., H. T. Lee, D. Rapoport, I. R. Drexler, K. Foster, J. Yang, K. M. Schmidt-Ott, X. Chen, J. Y. Li, S. Weiss, et al. 2005. Endocytic delivery of lipocalin-siderophore-iron complex rescues the kidney from ischemia-reperfusion injury. *J. Clin. Invest.* 115: 610–621.
35. Martineau, A. R., S. M. Newton, K. A. Wilkinson, B. Kampmann, B. M. Hall, N. Nawroly, G. E. Packe, R. N. Davidson, C. J. Griffiths, and R. J. Wilkinson. 2007. Neutrophil-mediated innate immune resistance to mycobacteria. *J. Clin. Invest.* 117: 1988–1994.
36. Sato, K., H. Tomioka, T. Shimizu, T. Gonda, F. Ota, and C. Sano. 2002. Type II alveolar cells play roles in macrophage-mediated host innate resistance to pulmonary mycobacterial infections by producing proinflammatory cytokines. *J. Infect. Dis.* 185: 1139–1147.
37. Bermudez, L. E., and J. Goodman. 1996. *Mycobacterium tuberculosis* invades and replicates within type II alveolar cells. *Infect. Immun.* 64: 1400–1406.
38. Garcia-Perez, B. E., R. Mondragon-Flores, and J. Luna-Herrera. 2003. Internalization of *Mycobacterium tuberculosis* by macropinocytosis in non-phagocytic cells. *Microb. Pathog.* 35: 49–55.
39. Adams, D. O., and T. A. Hamilton. 1984. The cell biology of macrophage activation. *Annu. Rev. Immunol.* 2: 283–318.
40. MacMicking, J., Q. W. Xie, and C. Nathan. 1997. Nitric oxide and macrophage function. *Annu. Rev. Immunol.* 15: 323–350.
41. Govoni, G., and P. Gros. 1998. Macrophage NRAMP1 and its role in resistance to microbial infections. *Inflamm. Res.* 47: 277–284.